Design and Simulation of Wideband Microstrip Components

Michael Knizek

Christopher Nicholl

Craig Popovich

Academic Advisor: Khair Al Shamaileh

Departments of Engineering
College of Engineering, Mathematics, and Sciences
Purdue University Northwest
April 26, 2017

Executive Summary

Front-end conventional microwave components such as antennas, couplers, and power dividers generally only operate at single frequencies. Because wireless communication is becoming more and more demanding, it is crucial that the designs of these elements evolve to operate at multiple frequencies. Doing so will allow greater functionality without sacrificing electrical performance, size, design complexity, and cost.

The team researched and designed two types of power dividers (Bagley and Wilkinson), and antennas (square patch). Using advanced simulation tools and other various types of software, the designs will be simulated for peak optimization. Once this was achieved, the final designs were fabricated.

More time was spent on the Bagley power dividers in order to familiarize the team with the required software tools, as well as the concepts being applied in the design process. Final results of the research on Bagley power divider's design was included in a conference paper detailing the design process of a miniaturized quad-band Bagley power divider which was accepted in the IEEE AP-S Symposium on Antennas and Propagation and USNC-URSI Radio Science Meeting in San Diego, California.

Abstract

Enhancement of conventional microwave front-end components will be achieved by utilizing modern design techniques and software simulation tools. The goal is to design front-end radio frequency microstrip components that can operate at multiple frequencies without sacrificing electrical performance, size, design complexity, and above all else, cost. The first semester was dedicated to designing and simulating a miniaturized quad band Bagley power divider and publishing the design process in an academic conference paper. The second semester focused on completing the designs and simulations of the Wilkinson power dividers, and square patch antennas. Also during the second semester, a handful of designs were fabricated for real world analysis to compare with simulated results.

Designing the components was split into multiple steps where different optimization techniques are used to add more operating frequencies, as well as decrease the size of the divider. The designs were drawn in Autodesk® AutoCAD® and simulated using ANSYS® Electronics Desktop. Similar steps were taken when working on Wilkinson power dividers and square patch antennas in the second semester. Parametric analysis was also applied to the antenna designs in order to fine tune the results to the team's specifications.

This project describes the process and methods used to design and optimize several unique microwave front-end components. It also presents the results obtained from simulation, as well as real world simulations from certain fabricated components for comparison.

Table of Contents

List of Tables

List of Figures

Introduction

Wireless communication technologies is becoming increasingly more demanding, and the conventional microwave components are inadequate to keep up with nowadays technological advances. Front-end components such as antennas, couplers, and power dividers generally only operate at single frequencies. Enhancement of such components will allow for wide or multiband functionality without sacrificing important factors and characteristics of the circuits.

Background

Microwave frequencies range between 300 MHz and 300 GHz. Examples of microwave technology include cellular communication, wireless local area networks (WLAN), satellite navigation, and radar. This project primarily focuses on cellular and WLAN frequencies (0.7-4.0 GHz) because of their domestic and commercial use in urban regions.

The components explored in this project are power dividers and antennas. A power divider receives power at its single input port and divides the power (evenly or unevenly, depending on the design) across its multiple output ports. A power combiner receives power through its multiple input ports and combines it at its single output port. In other words, power combiners and dividers are inverses of each other. The specific configurations of components that were designed are the Bagley power divider (BPD) and the Wilkinson power divider (WPD). The major difference between both dividers is that the isolation of the output ports of the Wilkinson power divider allows it to function as both a power divider and a combiner, while the Bagley power divider only functions as a divider. Antennas are used to convert radio waves into electric power (receiver), or to convert electric power into radio waves (transmitter). The type of antennas designed in this project are square patch antennas.

The components are designed using microstrip technology, which is a type of electrical transmission line that carries microwave frequency signals. Microstrip consists of a conductor, ground plane, and dielectric substrate, as seen in the figure below.

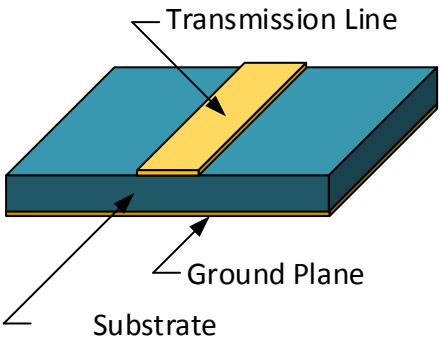

Figure 1. Microstrip Transmission Line Built on a Substrate.

Objectives

The goal of this project is to design, simulate, and fabricate front-end components and to verify their performance using a network analyzer. Conventional designs will be researched and verified, and then undergo modifications to allow for more complex operation. A paper will also be published detailing the process and results of one or more components designed in this project.

Constraints

Possibly the largest existing constraint was the fact that there were little to no related courses that the design team members could have taken to prepare them for most of the topics researched in this project. However, some courses such as MATLAB and Electromagnetics did offer some valuable information that was applied throughout the year.

Because the equipment here at Purdue University Northwest was too out of date to use, the team was required to travel to another university and make use of their advanced equipment. If the equipment located here was up to date, it could have saved the design team a fair amount of time and money.

The senior design team has received a $567.48 grant to be used toward the fabrication of three final circuit designs, submission cost of publishing a paper in a conference, the purchase of twelve interface connectors, and travel costs to visit the University of Akron in Akron, Ohio where advanced testing and measurements of the fabricated circuit designs was conducted. If additional funds were provided, more designs could have been fabricated and analyzed. The extra funds could also have funded another conference paper submission.

Given more time, the design team would have been able to expand the work on antennas similar to what was done with Bagley power dividers. Additional components

could have also been fabricated as well as 3D printed cases for said designs. Alternatively, these can make excellent tasks for a future design group.

Environmental Impact

The constant flow of microwave frequency waves creates a mild atmospheric heating effect, granted this happens over a very long exposure period. This effect is extremely minimal and hardly worth consideration for the small scale of this project. Because this project only focuses on small, individual components, their contribution to any kind of environmental effect is negligible.

In this project there was never a time where the fabricated components were operating in any form, aside from when the parameters were measured using the network analyzer. The network analyzer was operated in a controlled environment where none of the radio waves were subjected to the atmosphere.

Approach

The plan of work was divided into four stages, where within each stage it is assumed that the components of interest will go through a series of improvements through analytical design and software simulations. The stages are as follows:

1. Bagley power dividers
2. Wilkinson power dividers/combiners
3. Square Patch Antennas
4. Fabrication and measurements

The timeframe of this project can be referenced in **Appendix C**. All stages were completed by the current design team.

Bagley Power Dividers

Description: This involved designing and simulating conventional, compact, and multi-band Bagley power dividers using multi-section and coupled lines techniques. Three-way and five-way Bagley power dividers were designed to operate at various cellular and WLAN frequencies. Software tools used were ANSYS® Electronics Desktop 2016.1, Autodesk® AutoCAD® 2017, National Instruments™ TX-LINE, and MathWorks® MATLAB® R2016a.

This stage was divided into four activities.

Single-Band Bagley Power Dividers:

Initially, conventional Bagley power dividers were designed and simulated in order to learn about how they operate and what their downsides are. These are the simplest form of Bagley power dividers as they operate on only one frequency and take up a large amount of space. Subsequently, design techniques were applied to reduce the size of the circuits while maintaining satisfactory electrical performance.

The schematic diagram of a conventional three-way Bagley power divider is shown in Figure 2, and the five-way in Figure 3.

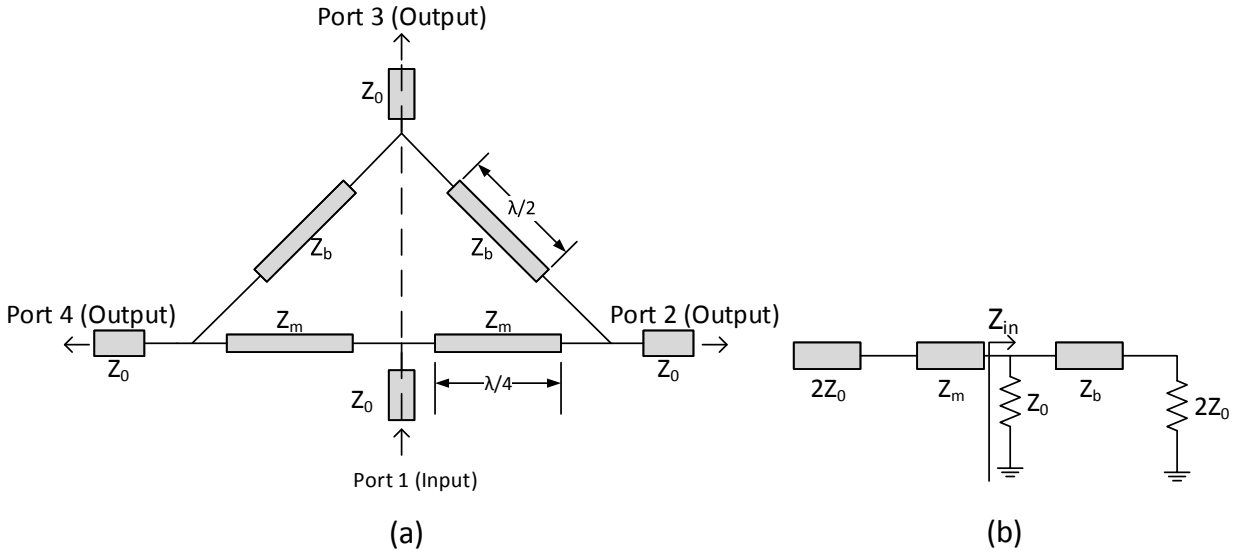

Figure 2. Conventional Three-Way BPD (a) Schematic Diagram and (b) Even-Mode Circuit.

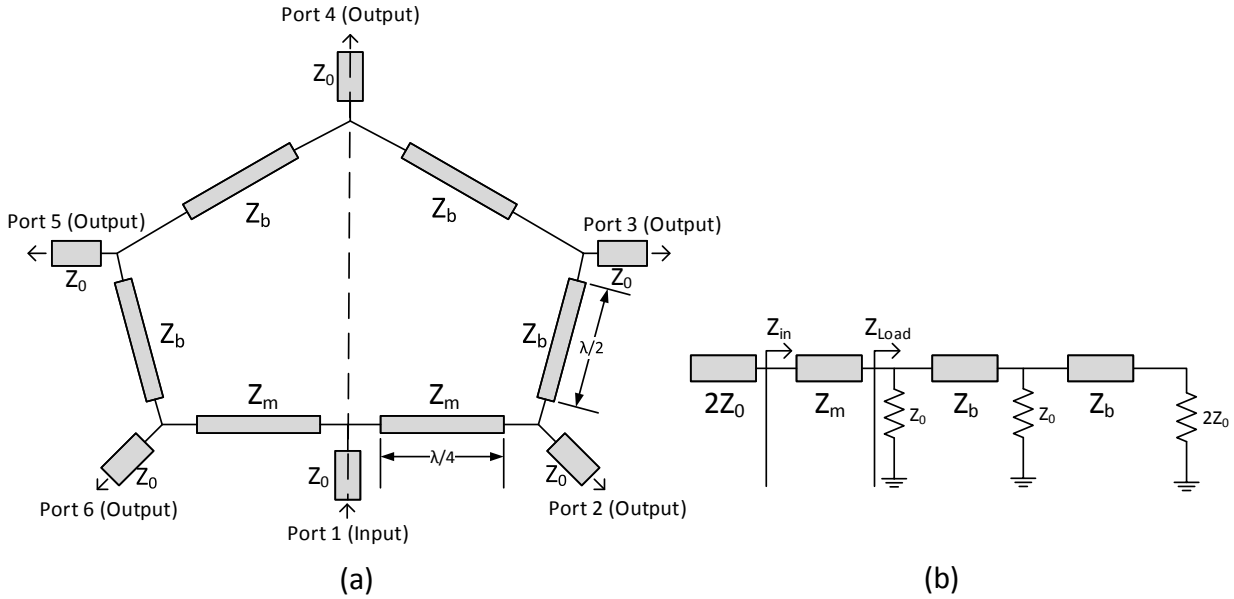

Figure 3. Conventional Five-Way BPD (a) Schematic Diagram and (b) Even-Mode Circuit.

As shown in Figure 2 and 3, Z_0, Z_m, and Z_b are the characteristic impedances of the corresponding transmission lines. Z_m, a quarter-wave transformer, has a length of $\lambda/4$, where λ is the guided wavelength. Z_b has a length of $\lambda/2$. Each transmission line also has a certain length and width that are derived from the operating frequency and impedance, respectively. In order to calculate the lengths, widths, and impedances, the even-mode circuits in Figure 1(b) and Figure 2(b) were analyzed.

As the length of Z_b is set to half-wave length, it will not affect the transformation process. As such, the input impedance, Z_{in} is the parallel combination of $2Z_0$ and Z_0. In general, for an N way power divder (N output ports):

$$Z_{in} = \frac{2}{N} Z_0$$

The quarter-wave transformer impedance Z_m is intended to match $Z_s = 2Z_0$ to Z_{in} using the well-known matching formula

$$Z_m = \sqrt{Z_S Z_{in}}$$

As such:

$$Z_m = \frac{2}{\sqrt{N}} Z_0$$

For the input and output ports, SMA (SubMiniature version A) connectors are used which have a standard characteristic impedance $Z_0 = 50\ \Omega$. Because the impedance of Line 'b' does not have an effect on impedance matching, it can be chosen arbitrarily. For convenience, Z_b was chosen to be equal to Z_m. Using the following equations, the width of the transmission line can be found [1].

$$\frac{W}{d} = \begin{cases} \dfrac{8e^A}{e^{2A}-2} & \text{for } \dfrac{W}{d} < 2 \\ \dfrac{2}{\pi}\left[B - 1 - \ln(2B-1) + \dfrac{\varepsilon_r + 1}{2}\left\{ \ln(B-1) + 0.39 - \dfrac{0.61}{\varepsilon_r} \right\} \right] & \text{for } \dfrac{W}{d} > 2 \end{cases}$$

$$A = \frac{Z_0}{60}\sqrt{\frac{\varepsilon_r + 1}{2}} + \frac{\varepsilon_r - 1}{\varepsilon_r + 1}\left(0.23 + \frac{0.11}{\varepsilon_r} \right)$$

$$B = \frac{377\pi}{2Z_0\sqrt{\varepsilon_r}}$$

For the substrate, FR-4 (Flame Retardant-4) epoxy was chosen which has a dielectric

constant (ε_r) of 4.6 and a substrate thickness (d) of 1.6 millimeters.

The length of the transmission line was derived from the following equations:
Effective dielectric constant:

$$\varepsilon_{eff} = \frac{\varepsilon_r + 1}{2} + \frac{\varepsilon_r - 1}{2} \frac{1}{\sqrt{1 + 12d / W}}$$

Where W is the width of the transmission line,

Electrical lengths:

$$\theta_b \equiv 180° \qquad \theta_m \equiv 90°$$

Physical lengths:

$$\lambda_b = \frac{c}{f\sqrt{\varepsilon_{eff}}} \rightarrow L_b = \frac{c}{2f\sqrt{\varepsilon_{eff}}}$$

$$\lambda_m = \frac{c}{f\sqrt{\varepsilon_{eff}}} \rightarrow L_b = \frac{c}{4f\sqrt{\varepsilon_{eff}}}$$

Where f is the design frequency and c is the speed of light, $3x10^8$ m/s.

The calculated impedances, widths, and lengths of the transmission lines for each frequency are shown in Tables 1 and 2.

Table 1. Calculated Values for Conventional Three-Way BPDs.

	0.870 GHz			1.96 GHz			2.13 GHz		
Line	Z (Ω)	W (mm)	L (mm)	Z (Ω)	W (mm)	L (mm)	Z (Ω)	W (mm)	L (mm)
o	50.000	2.959	10.000	50.000	2.959	10.000	50.000	2.959	10.000
b	57.735	2.306	93.651	57.735	2.306	41.569	57.735	2.306	38.252
m	57.735	2.306	46.825	57.735	2.306	20.785	57.735	2.306	19.126

Table 2. Calculated Values for Conventional Five-Way BPDs.

	0.870 GHz			1.96 GHz			2.13 GHz		
Line	Z (Ω)	W (mm)	L (mm)	Z (Ω)	W (mm)	L (mm)	Z (Ω)	W (mm)	L (mm)
o	50.000	2.959	10.000	50.000	2.959	10.000	50.000	2.959	10.000
b	44.721	3.554	92.010	44.721	3.554	40.841	44.721	3.554	37.581
m	44.721	3.554	46.005	44.721	3.554	20.421	44.721	3.554	18.791

Using ANSYS Electronics Desktop, the designs were verified by the circuit analysis tool,

ANSYS Designer. Designer was used to quickly create a simple version of the circuit and run a basic analysis to confirm the numerical analysis validity. Figure 4 shows the circuit and analysis results for a conventional three-way Bagley power divider operating at 0.870 GHz. The resulting S-parameters show that there is a frequency matching at the design frequency, characterized by an input port matching parameter (S_{11}) of –40 dB and transmission parameters, S_{21}, S_{31}, and S_{41} of –4.7 dB. The next step involves full-wave simulations as will be elaborated.

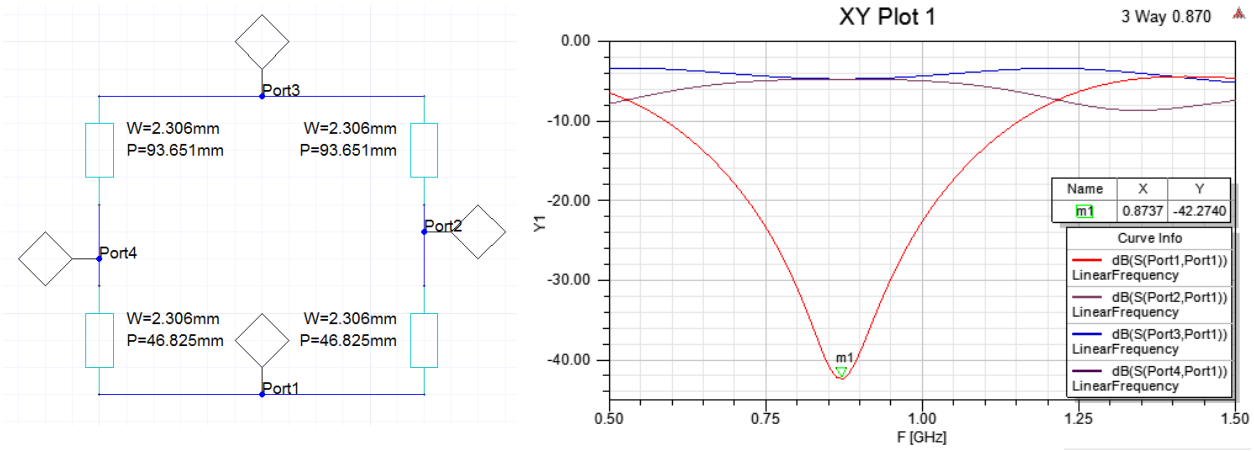

(a) (b)

Figure 4. ANSYS Designer (a) Circuit model and (b) Analysis results at 0.870 GHz.

After confirming the results of various power dividers operating at different frequencies, the designs were drawn using Autodesk AutoCAD. The drawings created in AutoCAD were imported into the HFSS (High Frequency Structural Simulator) full-wave simulation tool in ANSYS Electronics Desktop. Three-dimensional models of the power dividers were created in HFSS, as shown in Figure 5. The green box is the substrate; whereas the purple lines are the designed transmission lines. The input and output ports are defined by the rectangles touching the edges of the substrate.

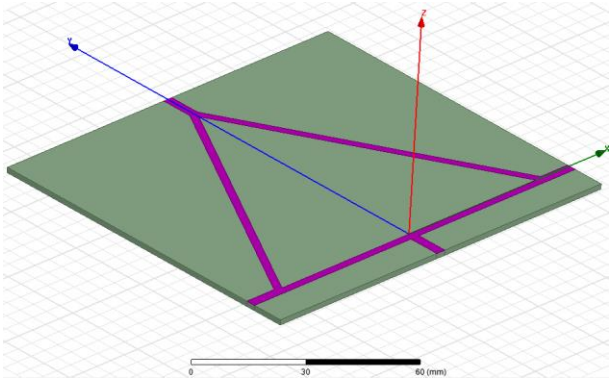

Figure 5. Three-Dimensional Model Created in HFSS.

HFSS considers electromagnetic effects and phenomena (e.g., conductor and dielectric losses) that Designer does not. The simulated results for the three-way and five-way conventional Bagley Power dividers operating at 1.96 GHz are shown in Figures 9 and 10 respectively, which display the scattering parameters as a function of frequency versus magnitude. The scattering parameter, denoted as S*ij*, is defined as the power transmitted to port *j* provided that port *i* is fed. For example, S_{21} is the power transmitted to Port 2 (output port) given that Port 1 (input port) is excited. On the other hand, S_{ii} indicates the power reflected back at Port *i*. In order to verify the results of each power divider, S_{11} should have a minimal magnitude at the designated frequency. For example, Figure 6 shows the simulated input port matching (S_{11}) and transmission parameters (S_{21}, S_{31}, S_{41}, S_{51}, S_{61}). Input port matching is less than -20 dB at the design frequency, 1.96 GHz, whereas the transmission parameters are in proximity to their theoretical value of -4.7 dB and –6.9 dB, for the 3- and 5-way dividers, respectively, at 1.96 GHz. The rest of the simulated results for the conventional Bagley power dividers at different frequencies are found in **Appendix A**.

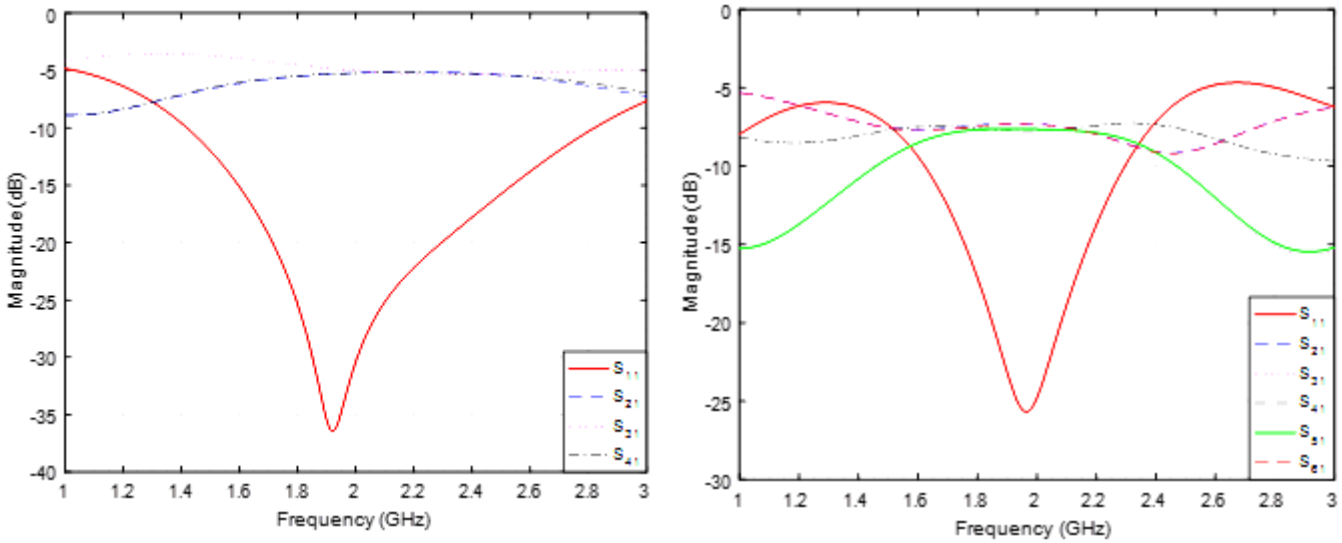

(a) (b)

Figure 6. S-Parameters of Conventional (a) Three-Way and (b) Five-Way BPDs operating at 1.96 GHz.

After confirming the functionality of conventional Bagley power dividers, the designs needed to be modified to be smaller without sacrificing performance. The same 3- and 5-way configurations were designed at the same frequencies as before, but the size of the circuits was reduced significantly. The modified 3-way Bagley power divider can be modeled as shown in Figure 7.

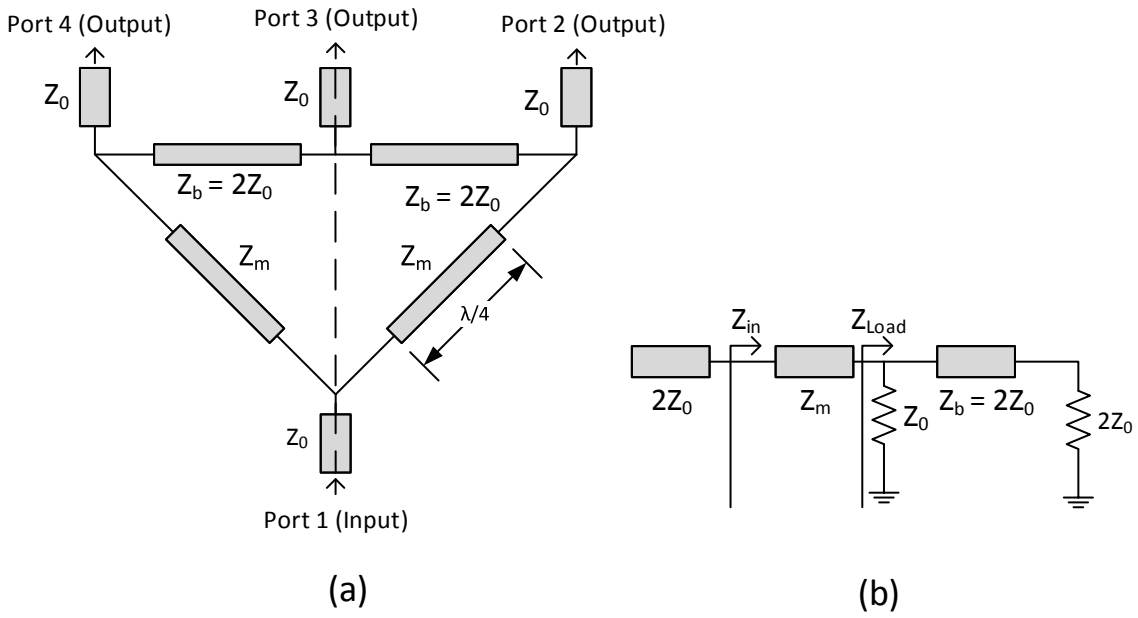

Figure 7. Modified Three-Way BPD (a) Schematic Diagram and (b) Even-Mode Circuit

The modified five-way Bagley power divider can be modeled as seen in the figure below.

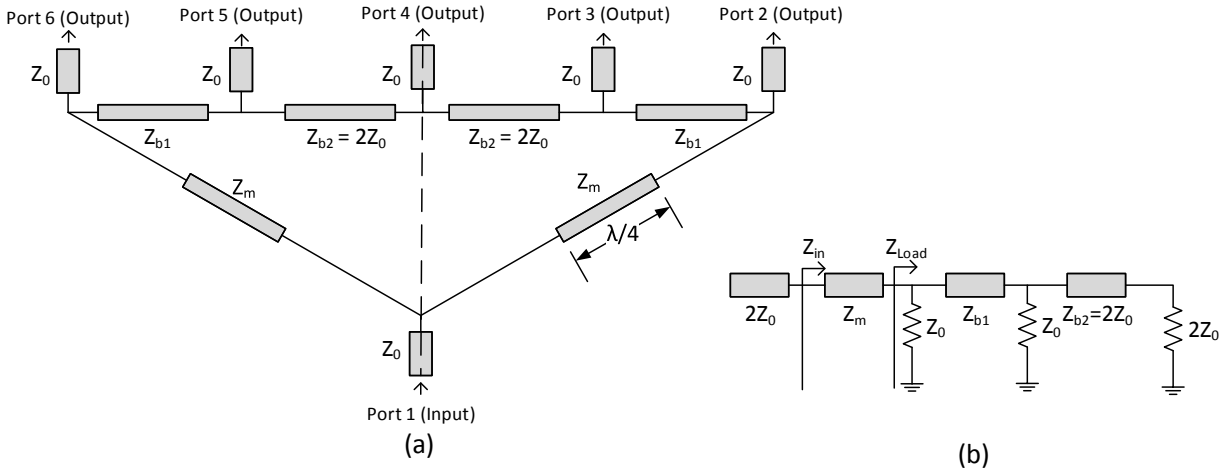

Figure 8. Modified Five-Way BPD (a) Schematic Diagram and (b) Even-Mode Circuit

Analysis of the modified models followed the same procedure as in the conventional Bagley power dividers, and the same equations were used to calculate the impedances, widths, and lengths of the transmission lines. The only difference was that by making Z_b equals $2Z_0$, the length of Z_b (Z_{b1} and Z_{b2} for the five-way) can be arbitrarily chosen [2]. This allowed the size of the circuit to be significantly reduced. The calculated values are displayed in the Tables 3 and 4.

Table 3. Calculated Values for Modified Three-Way BPDs.

	0.870 GHz			1.96 GHz			2.13 GHz		
Line	Z (Ω)	W (mm)	L (mm)	Z (Ω)	W (mm)	L (mm)	Z (Ω)	W (mm)	L (mm)
o	50.000	2.959	10.000	50.000	2.959	10.000	50.000	2.959	10.000
b	100.000	0.672	(Arbitrary)	100.000	0.672	(Arbitrary)	100.000	0.672	(Arbitrary)
m	57.735	2.306	46.825	57.735	2.306	20.785	57.735	2.306	19.126

Table 4. Calculated Values for Modified Five-Way BPDs.

	0.870 GHz			1.96 GHz			2.13 GHz		
Line	Z (Ω)	W (mm)	L (mm)	Z (Ω)	W (mm)	L (mm)	Z (Ω)	W (mm)	L (mm)
0	50.000	2.959	10.000	50.000	2.959	10.000	50.000	2.959	10.000
b1	33.333	5.517	(Arbitrary)	33.333	5.517	(Arbitrary)	33.333	5.517	(Arbitrary)
b2	100.000	0.672	(Arbitrary)	100.000	0.672	(Arbitrary)	100.000	0.672	(Arbitrary)
m	44.721	3.554	46.005	44.721	3.554	20.421	44.721	3.554	18.791

The calculated values were again used in ANSYS Designer to verify them, and then used for in HFSS simulations. Figures 9a and 9b once again show the input port matching and transmission parameters of the simulated circuits. Magnitudes of at least -20 dB or less are present at the design frequencies, which confirmed that the modified Bagley power dividers retain their performance (Refer to **Appendix A** for more results).

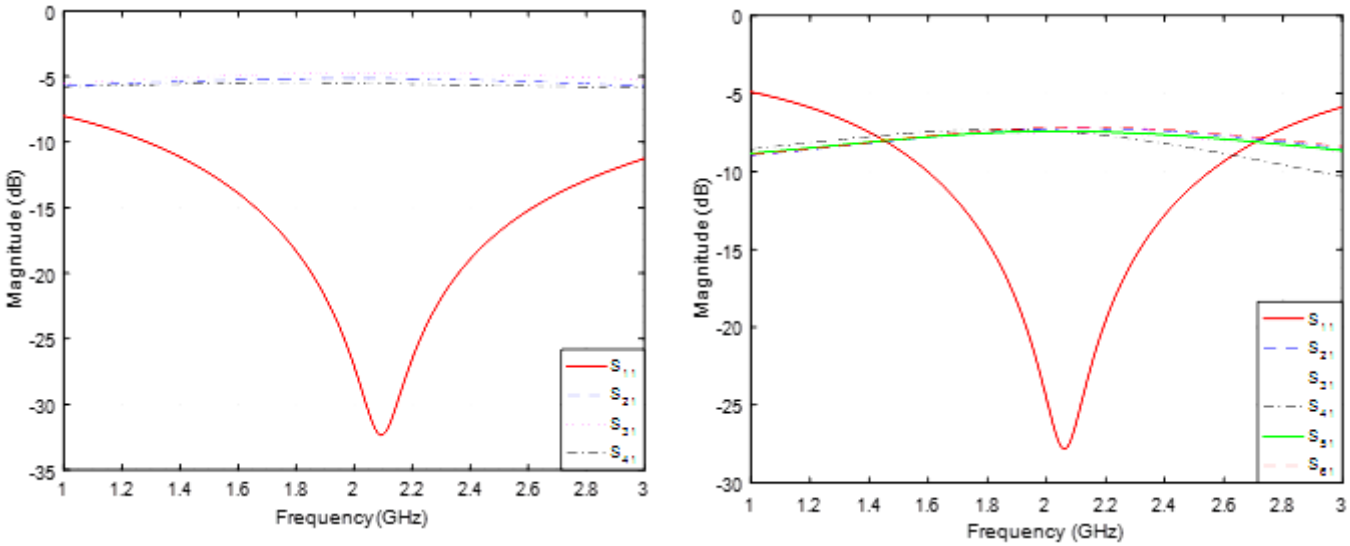

(a) (b)

Figure 9. S-Parameters of Modified (a) Three-Way and (b) Five-Way BPDs at 2.13 GHz.

Dual-Band Bagley Power Dividers:

The next step was to extend the designs of the modified Bagley power dividers to operate at two different frequencies simultaneously.

The designs had similar layouts to the modified power dividers, but multi-section transmission lines were employed for dual-band functionality to occur. The dual-band three-way and five-way Bagley power divider models are shown in Figures 10 and 11.

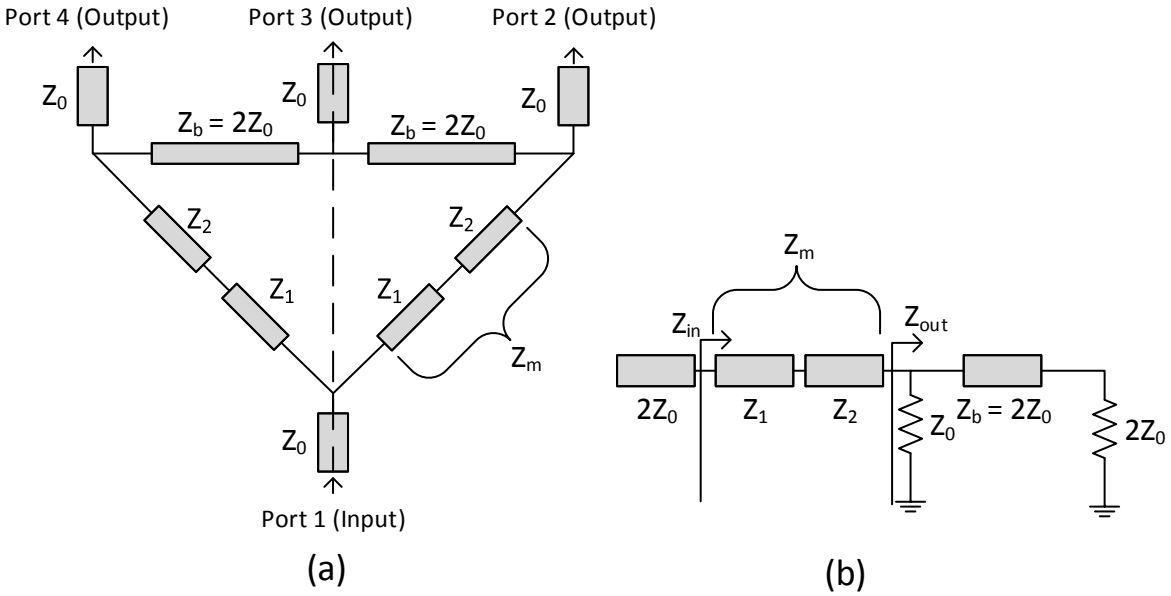

Figure 10. Dual-Band Three-Way BPD (a) Schematic Diagram and (b) Even-Mode Circuit.

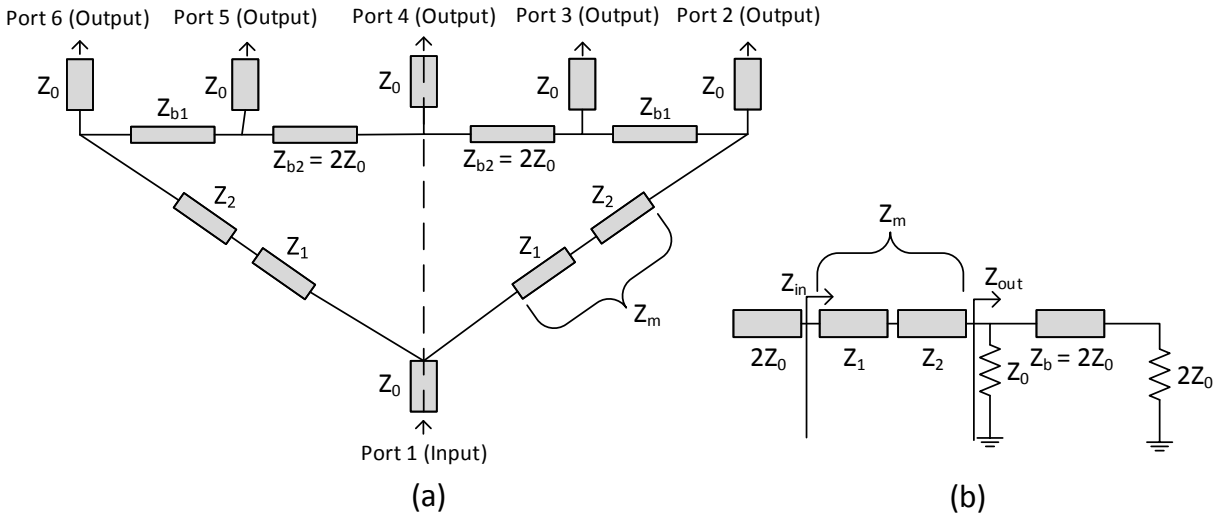

Figure 11. Dual-Band Five-Way BPD (a) Schematic Diagram and (b) Even-Mode Circuit.

For dual-band operation, Z_m was replaced by two cascaded lines with different widths.

The widths and lengths of Z_1 and Z_2 were calculated by utilizing Monzon's Theorem of dual-band operation, which is summarized in the equations below [3]:

Given that:

$$Z_{in} = 2Z_0$$

$$Z_{out} = \frac{2}{3}Z_0$$

The impedances of Z_1 and Z_2 are calculated by

$$Z_1 = \sqrt{\frac{Z_{in}}{2\alpha}\left(Z_{out} - Z_{in}\right) + \sqrt{\left(\frac{Z_{in}}{2\alpha}\left(Z_{out} - Z_{in}\right)\right)^2 + Z_{in}{}^3 Z_{out}}}$$

$$Z_2 = \frac{Z_{in}Z_{out}}{Z_1}$$

Where α is derived from:

$$\alpha = \tan^2\left(\beta_1 l\right)$$

$$l = \frac{\pi}{\beta_1 + \beta_2}$$

$$\beta_n = \frac{2\pi}{\lambda_n}$$

$$\lambda_n = \frac{c}{f_n\sqrt{\varepsilon_{eff}}}$$

The calculated values of the transmission lines are shown in the tables below.

Table 5. Calculated Values, Dual-Band Three-Way BPD.

0.870 GHz + 2.13 GHz				0.870 GHz + 1.96 GHz			1.96 GHz + 2.13 GHz		
Line	Z (Ω)	W (mm)	L (mm)	Z (Ω)	W (mm)	L (mm)	Z (Ω)	W (mm)	L (mm)
o	50.000	2.959	10.000	50.000	2.959	10.000	50.000	2.959	10.000
b	100.000	0.672	(Arbitrary)	100.000	0.672	(Arbitrary)	100.000	0.672	(Arbitrary)
1	64.081	1.897	27.159	66.299	1.775	28.790	75.890	1.338	19.921
2	52.018	2.768	27.159	50.277	2.931	28.790	43.923	3.657	19.921

Table 6. Calculated Values, Dual-Band Five-Way BPD.

0.870 GHz + 2.13 GHz				0.870 GHz + 1.96 GHz			1.96 GHz + 2.13 GHz		
Line	Z (Ω)	W (mm)	L (mm)	Z (Ω)	W (mm)	L (mm)	Z (Ω)	W (mm)	L (mm)
o	50.000	2.959	10.000	50.000	2.959	10.000	50.000	2.959	10.000
b1	33.333	5.517	(Arbitrary)	33.333	5.517	(Arbitrary)	33.333	5.517	(Arbitrary)
b2	100.000	0.672	(Arbitrary)	100.000	0.672	(Arbitrary)	100.000	0.672	(Arbitrary)
1	51.690	2.798	26.683	54.326	2.569	28.286	66.746	1.751	19.572
2	38.692	4.442	26.683	36.815	4.781	28.286	29.964	6.398	19.572

The designs were analyzed and simulated using ANSYS Designer and HFSS, respectively. Figures 12a and 12b (and the results in **Appendix A**) show the simulated results of the dual-band designs. For each plot, input port matching at two distinct frequencies of at least -20 dB can be seen. The results proved that dual-band functionality was achieved.

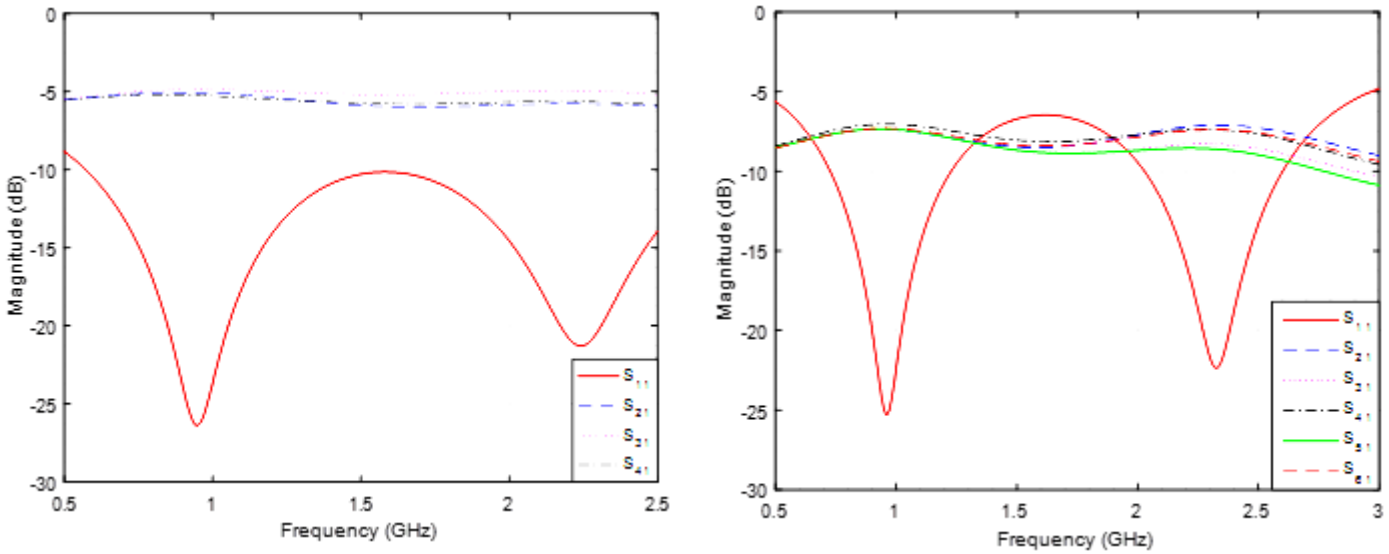

(a) (b)

Figure 12. S-Parameters of Dual-Band (a) Three-Way and (b) Five-Way BPDs at 0.870 and 2.13 GHz.

Tri-Band and Quad-Band Bagley Power Dividers:

The designs of the Bagley power dividers were extended further for operation at three or four frequencies. Like the dual-band designs, the models for the tri-band and quad-band dividers also contain multi-section lines as shown in the figure below. A new substrate, RT5880 which has a dielectric constant of 2.2 and substrate height of 0.787 millimeters, was chosen for its ability to better handle losses at higher frequencies. New design frequencies were also chosen, which were 0.73, 1.65, 2.67, and 3.57 GHz.

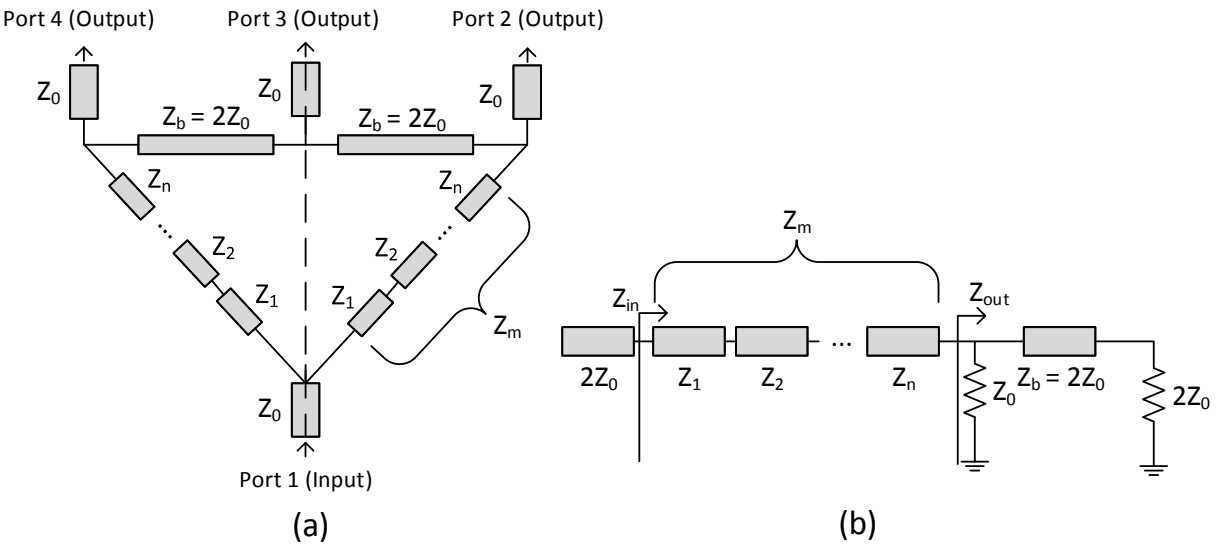

Figure 13. n-Band Three-Way BPD (a) Schematic Diagram and (b) Even-Mode Circuit.

It is noteworthy to point out that there are no exact formulas for the design of the impedances and lengths of the three-section transmission line. As such an optimization process was performed in MATLAB to find the optimum impedances and lengths of all sections using "fmincon". This was done by setting an objective function to find the optimum values for widths and lengths of the lines within specified design constraints and bounds. The code was run iteratively until the error function was acceptably low enough [4]. Refer to **Appendix D** for the full MATLAB code.

The *ABCD* matrix of a section with length l_i (i = number of sections) at frequency f_k (k = number of frequencies) can be given as:

$$\begin{bmatrix} A_{ik} & B_{ik} \\ C_{ik} & D_{ik} \end{bmatrix}_{Z_i} = \begin{bmatrix} \cos(\theta_{ik}) & jZ_i \sin(\theta_{ik}) \\ jZ_i^{-1} \sin(\theta_{ik}) & \cos(\theta_{ik}) \end{bmatrix}$$

where θ_{ik} is the electrical length of the i^{th} section given as:

$$\theta_{ik} = 2\pi \left(\frac{l_i f_k \sqrt{\varepsilon_{eff}}}{c} \right)$$

ε_{eff} is the effective dielectric constant, and c is the speed of light. The ABCD matrix of the three-section line at f_k is found by multiplying the *ABCD* matrix of each section:

$$ABCD_k = \begin{bmatrix} A_{1k} & B_{1k} \\ C_{1k} & D_{1k} \end{bmatrix} \cdot \begin{bmatrix} A_{2k} & B_{2k} \\ C_{2k} & D_{2k} \end{bmatrix} \cdot \begin{bmatrix} A_{3k} & B_{3k} \\ C_{3k} & D_{3k} \end{bmatrix}$$

Or in the case of four-sections:

$$ABCD_k = \begin{bmatrix} A_{1k} & B_{1k} \\ C_{1k} & D_{1k} \end{bmatrix} \cdot \begin{bmatrix} A_{2k} & B_{2k} \\ C_{2k} & D_{2k} \end{bmatrix} \cdot \begin{bmatrix} A_{3k} & B_{3k} \\ C_{3k} & D_{3k} \end{bmatrix} \cdot \begin{bmatrix} A_{4k} & B_{4k} \\ C_{4k} & D_{4k} \end{bmatrix}$$

The input impedance, Z_{in}, is calculated by

$$Z_{in}\left(f_k\right) = \frac{ABCD_k\left(1,1\right)\cdot Z_l + ABCD_k\left(1,2\right)\cdot Z_l}{ABCD_k\left(2,1\right)\cdot Z_l + ABCD_k\left(2,2\right)\cdot Z_l}$$

where $Z_l = 2Z_0 / 3$. Upon determining Z_{in} at f_k, the input reflection coefficient, $\Gamma_{in}(f_k)$ is

$$\Gamma_{in}\left(f_k\right) = \frac{Z_{in}\left(f_k\right) - 2Z_0}{Z_{in}\left(f_k\right) + 2Z_0}$$

For a perfect input port matching at the design frequencies, Γ_{in} at f_k should be zero (or very small). Thus, the following error function is minimized considering the impedance of each section is between 20Ω and 100Ω, the length of each section is between 5mm and 30mm, and using the RT5880 substrate thickness of 0.787 mm and relative permittivity of 2.2.

$$Error = \sum_{k=1}^{n} \left|\Gamma_{in}\left(f_k\right)\right|^2$$

A flowchart that summarizes the process of the MATLAB code is shown in the figure below.

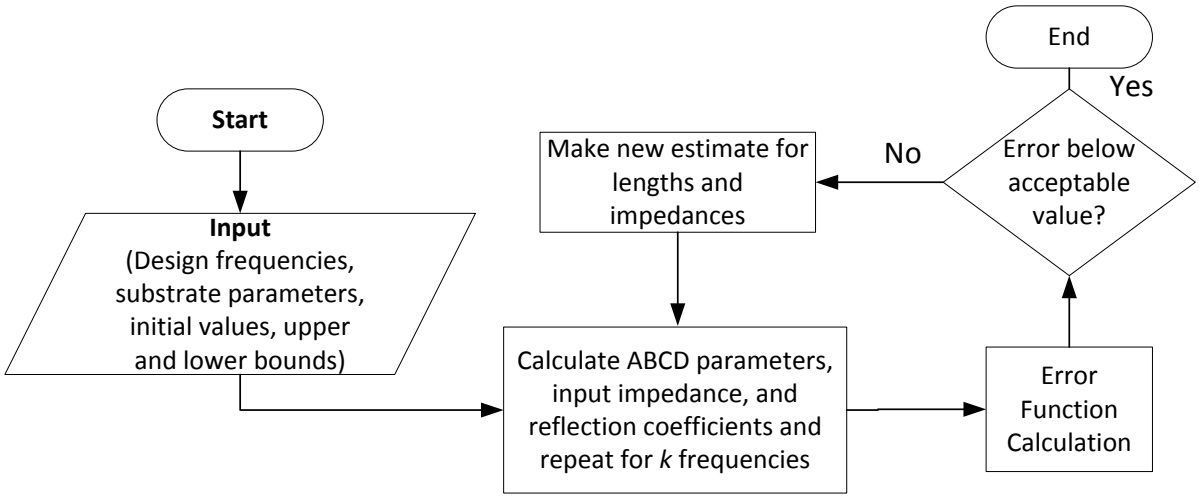

Figure 14. MATLAB Flowchart for Calculation of n-Band Line Values.

The values for the widths and lengths obtained from the MATLAB code are listed in the tables below.

Table 7. Calculated Values for Three-Way Tri-Band BPD.

0.73 GHz + 1.65 GHz + 2.67 GHz			
Line	Z (Ω)	W (mm)	L (mm)
o	50.000	2.425	10.000
b	100.000	0.705	(Arbitrary)
1	69.881	1.420	34.600
2	57.735	1.943	29.900
3	47.700	2.600	34.000

Table 8. Calculated Values for Three-Way Quad-Band BPD.

0.73 GHz + 1.65 GHz + 2.67 GHz + 3.57 GHz			
Line	Z (Ω)	W (mm)	L (mm)
o	50.000	2.425	10.000
b	100.000	0.705	(Arbitrary)
1	73.110	1.311	25.600
2	62.870	1.693	26.000
3	53.020	2.220	25.800
4	45.500	2.785	25.000

The designs were analyzed and simulated in ANSYS Electronics Desktop, and the simulated results are displayed in Figure 15.

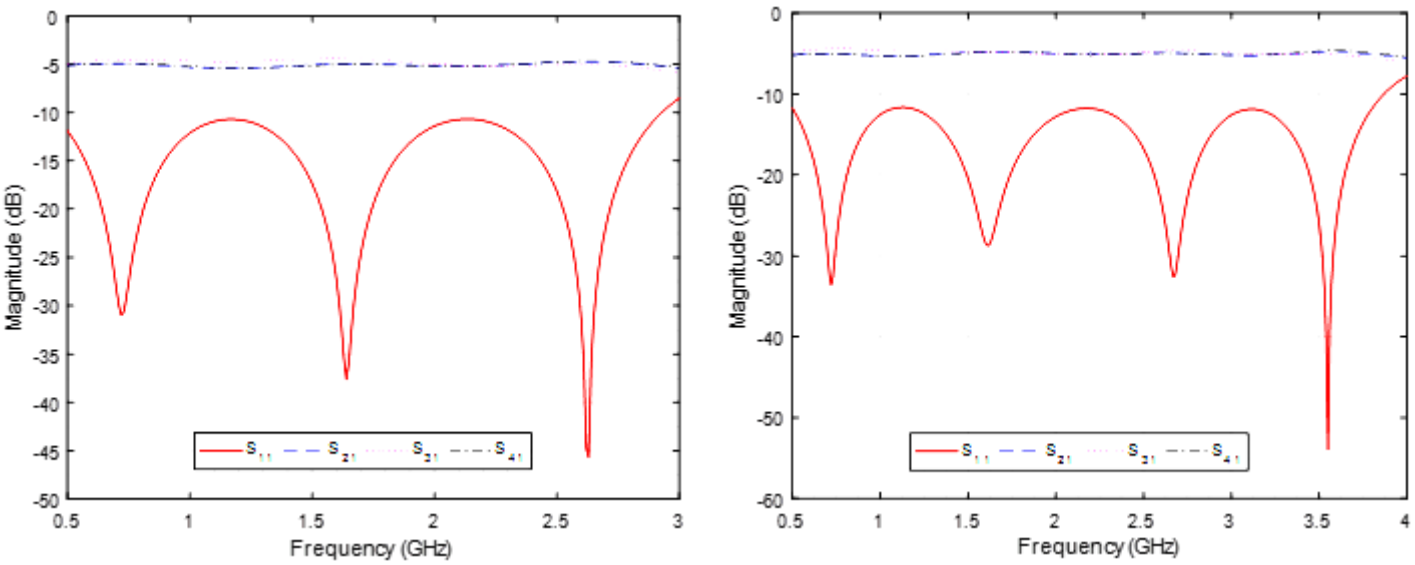

(a) (b)

Figure 15. S-Parameters of (a) Three-Way Tri-Band BPD at 0.730, 1.65, and 2.67 GHz (b) Three-Way Quad-Band BPD at 0.730, 1.65, 2.67, and 3.57 GHz.

The plots demonstrate the power divider's ability to operate at four different frequencies at once. However, the surface area of the circuits has been significantly increased as compared to the single-band Bagley power divider. A size comparison between the three-way quad-band Bagley power divider and a conventional single-band Bagley

power divider is shown in Figure 16.

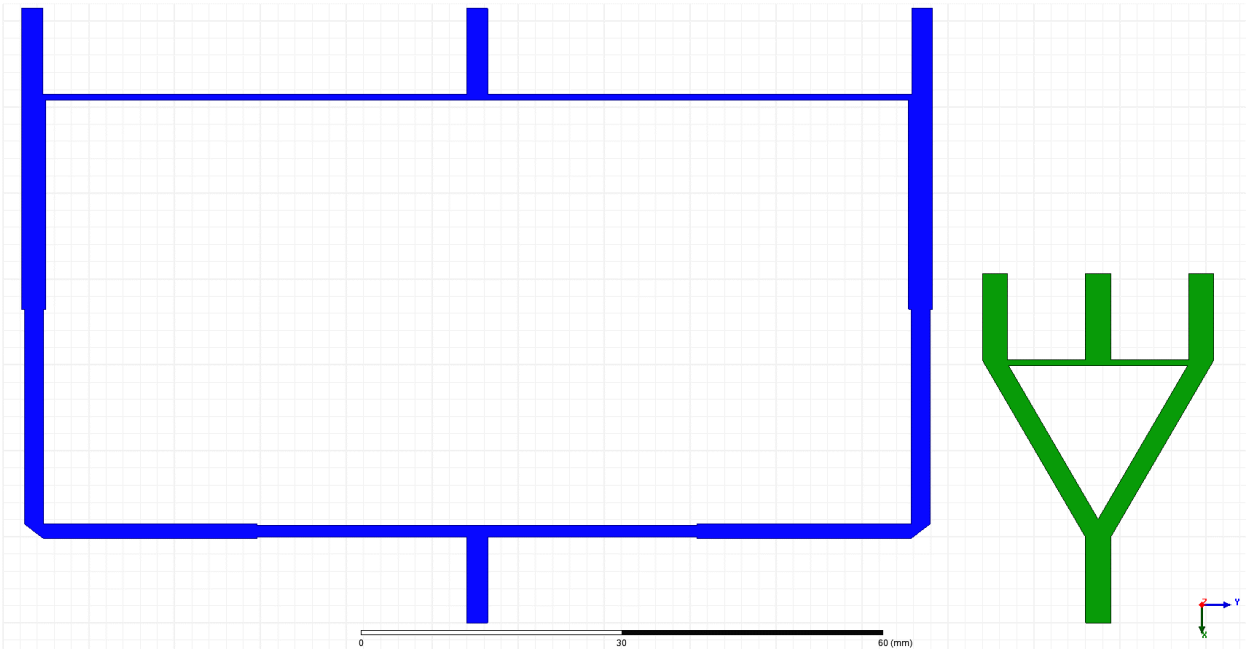

Figure 16. Size Comparison of (a) Quad-Band BPD and (b) Single-Band BPD.

Miniaturized Quad-Band Bagley Power Divider:

Following the completion of the traditional quad-band circuit, reducing the size of the three-way power divider was explored. This was accomplished using T-section coupled line networks. Coupling between transmission lines occurs when they are in close enough proximity to one another so that energy passes from one to the other through electromagnetic means. In most circumstances coupling between lines is undesirable, but by properly utilizing this phenomenon it can be used to condense transmission line lengths and allow for multi-frequency operation. A model of the circuit is shown in the figure below.

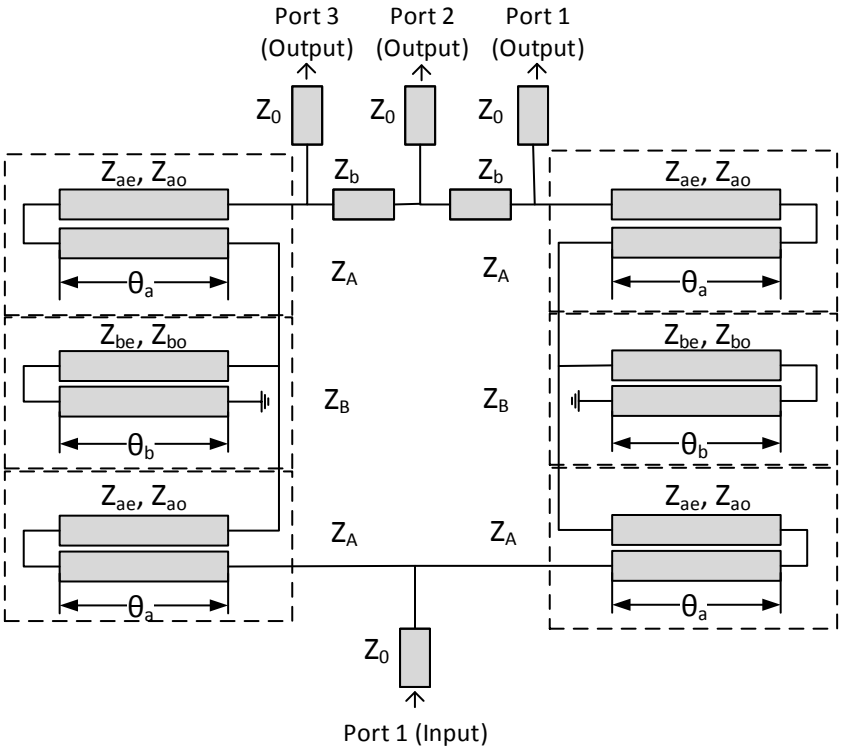

Figure 17. Schematic Diagram of the Miniaturized Quad-Band BPD Using Coupled Lines.

The impedance of the quarter wavelength transformer in this case is equivalent to a T-section comprised of Z_A, Z_B, and another Z_A. Within Z_A and Z_B is a pair of coupled lines, denoted as Z_{ae} and Z_{ao} in Z_A and Z_{be} and Z_{bo} in Z_B. Z_{ae} and Z_{be} are the even mode impedances of their pair and Z_{ao} and Z_{bo} are the odd mode impedances of their pair. The characteristic impedance of each pair, Z_A and Z_B, are calculated by [5]:

$$Z_A = \sqrt{Z_{ae} \cdot Z_{ao}}$$

$$Z_B = \sqrt{Z_{be} \cdot Z_{bo}}$$

The impedance of each coupled line was calculated by the following equations:

$$Z_{ae} = \left(\frac{\tan(\theta_2) - \tan(\theta_1)}{2} \right) \cdot \frac{2Z_0}{\sqrt{N}}$$

$$Z_{ao} = \left(\frac{\tan(\theta_2) - \tan(\theta_1)}{2\tan(\theta_1)\tan(\theta_2)} \right) \cdot \frac{2Z_0}{\sqrt{N}}$$

$$Z_{be} = \left(\frac{\tan(\theta_2) - \tan(\theta_1)}{2} \right) \cdot \left(\frac{Z_A{}^2}{Z_C{}^2 - Z_A{}^2} \right) \cdot \frac{2Z_0}{\sqrt{N}}$$

$$Z_{bo} = \left(\frac{\tan(\theta_2) - \tan(\theta_1)}{2\tan(\theta_1)\tan(\theta_2)} \right) \cdot \left(\frac{{Z_A}^2}{{Z_C}^2 - {Z_A}^2} \right) \cdot \frac{2Z_0}{\sqrt{N}}$$

where the electrical length of each coupled line is

$$\theta_i = \frac{f_i}{2f_0}$$

Given that

$$f_0 = \frac{f_1 + f_4}{2} = \frac{f_2 + f_3}{2}$$

Once the even-mode and odd-mode impedances were known, widths, lengths, and line separations were found using National Instruments TX-Line coupled line calculator. Further optimizations of the values were done to fine-tune the simulated results. The lengths, widths, and separations are shown in the table below.

Table 9. Calculated Values for Quad-Band BPD Using Coupled Lines.

Line	Z (Ω)	W (mm)	L (mm)	S (mm)
Z_{ae}	70.900	2.640	17.300	0.470
Z_{ao}	44.400			
Z_{be}	120.300	2.410	22.300	0.720
Z_{bo}	75.400			

The circuit was drawn in AutoCAD and imported into HFSS. The simulated results are shown below.

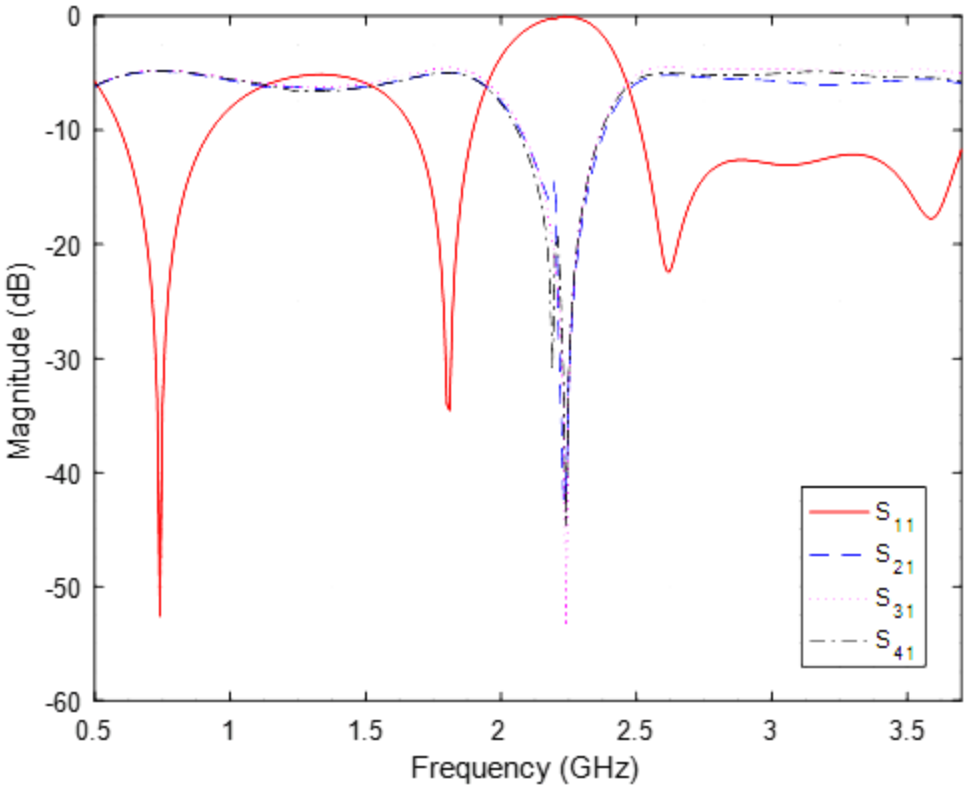

Figure 18. S-Parameters of Quad-Band BPD Using Coupled Lines at 0.73, 1.65, 2.67, and 3.57 GHz.

The results show that input return loss better than -15 dB was achieved, and the transmission parameters were within -4.77 dB tolerance. The use of the coupled line technique resulted in a size reduction of 62%, as seen in the figure below.

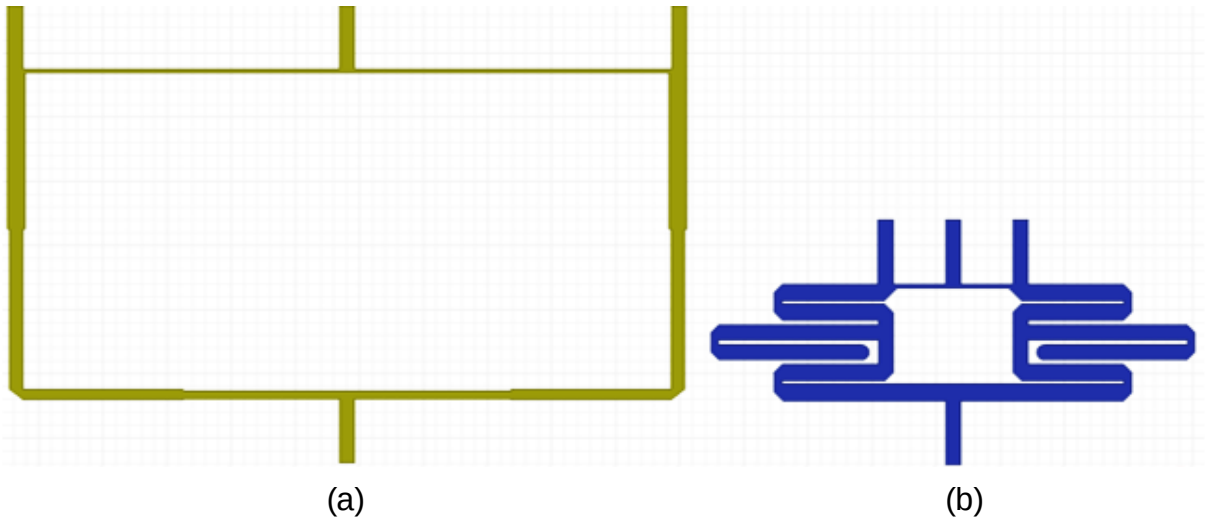

Figure 19. Comparison of Quad-Band BPDs using (a) Multi-Sectioning and (b) Coupled Lines.

The process and results of the miniaturized quad-band Bagley power divider was submitted to the 2017 IEEE AP-S/URSI Conference and accepted for publication. The conference paper can be found in **Appendix C**.

Wilkinson Power Dividers/Combiners

Description: This involved designing and simulating single-band, wideband, and unequal split Wilkinson power dividers using multi-section transmission lines and open stubs. They were designed around similar frequencies used by the Bagley power dividers, and the same software tools were used. All of the following Wilkinson power dividers used the RO4003C substrate which has a thickness of 0.813 millimeters and a dielectric constant of 3.55. Surface mount device (SMD) resistors which were 1.25 millimeters in length and 2.0 millimeters wide were used.

This stage was divided into three activities.

Single-Band Wilkinson Power Dividers:

The simplest form of Wilkinson power dividers was examined to understand the design procedure and operation of the device. The Wilkinson power divider operates similarly to the Bagley power divider, but the inclusion of a resistor before the output ports isolates them and allows it to operate as a power combiner. In the case of a conventional Wilkinson power divider, the isolation resistor always had a value of 100Ω. A model of the design is shown in the figure below.

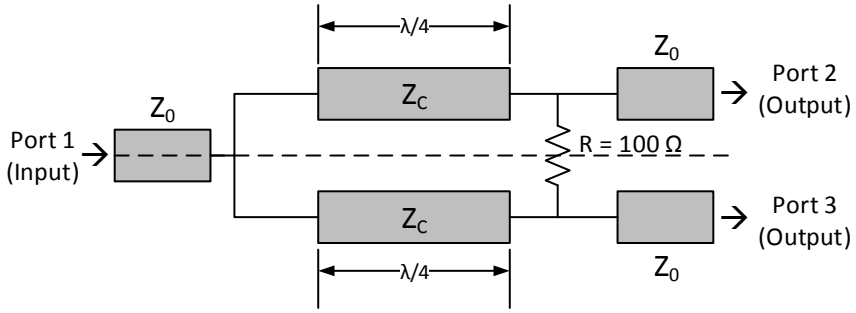

Figure 20. Schematic Diagram of Conventional WPD.

To design this, the even-mode circuit and odd-mode circuit must be analyzed individually, seen in the figure below.

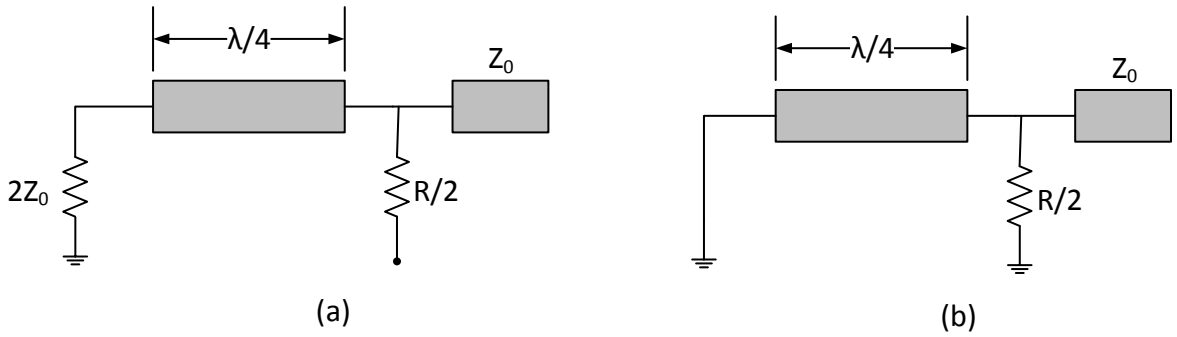

Figure 21. Conventional WPD (a) Even-Mode Circuit and (b) Odd-Mode Circuit.

Then the characteristic impedance of the quarter-wave transformer is derived from [6]

$$Z_C = \sqrt{Z_S Z_L} = \sqrt{2Z_0 Z_0} = \sqrt{2}Z_0$$

Given that

$$Z_S = 2Z_0 = 100\Omega$$

$$Z_L = Z_0 = 50\Omega$$

Since Z_C is the only impedance that needs to be calculated, creating a conventional Wilkinson power divider is simple. The values for a Wilkinson power divider with an operating frequency of 1.0 GHz is shown in the table below.

Table 10. Calculated Values for Conventional WPD at 1.0 GHz.

Line	Z (Ω)	W (mm)	L (mm)
o	50.000	1.819	10.000
C	70.711	0.992	45.965

Drawn in AutoCAD and imported into HFSS, the design was simulated. However, when testing the operating of a Wilkinson power divider the output port matching and isolation S-parameters as well as the input port matching and transmission S-parameters must be plotted. The simulated results of the 1.0 GHz design are shown in the plots below. The input/output port matching measures less than -20 dB and the transmission parameters around -3.2 dB which is in very close proximity to the theoretical value of -3 dB. S_{33} and S_{31} also equals to S_{22} and S_{21}, respectively due to structural symmetry.

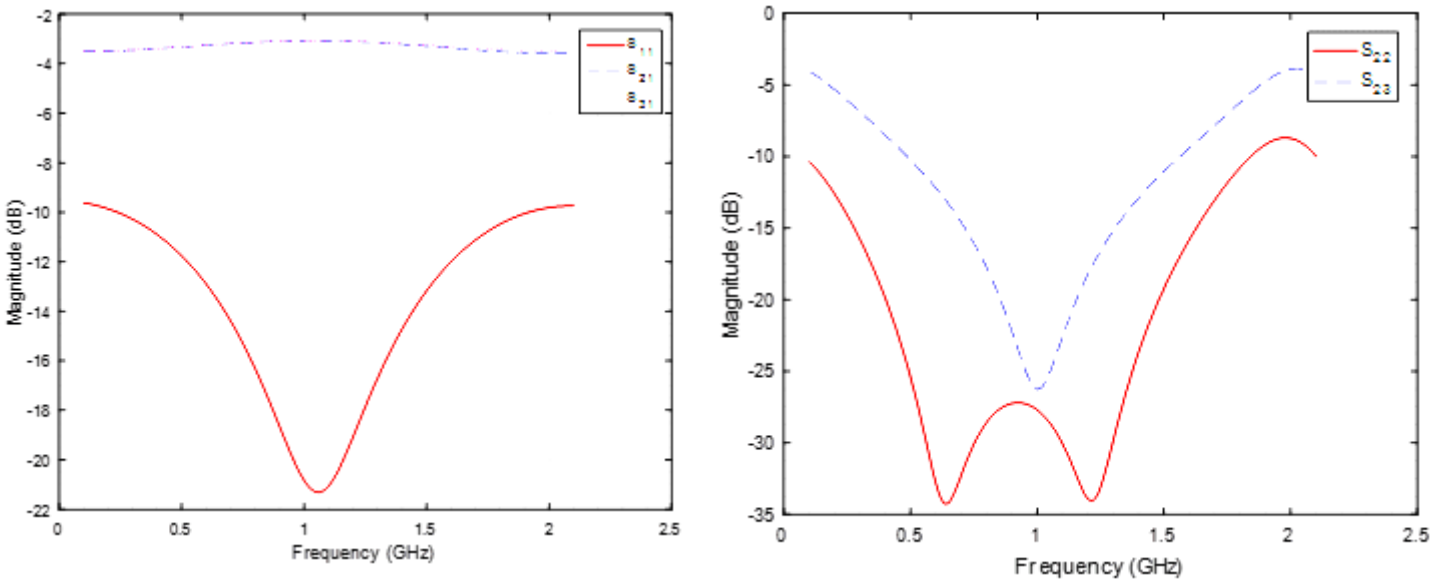

(a) (b)

Figure 22. S-Parameters of Conventional WPD (a) Input Port Matching and Transmission and (b) Output Port Matching and Isolation at 1.0 GHz.

Wideband Wilkinson Power Divider:

By utilizing multi-section transmission lines, wideband operation was achieved for the Wilkinson power divider. Instead of targeting a specific number of unique frequencies, wideband refers to all of the frequencies in between two different frequencies. A wideband Wilkinson power divider with *n* sections is shown in the model below.

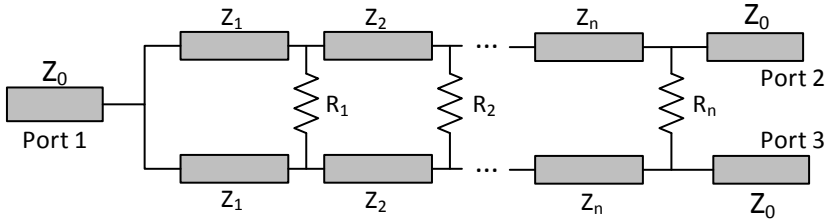

Figure 23. Schematic Diagram of Wideband WPD with n-Sections.

Similarly to the tri-band and quad-band Bagley power dividers, standardized equations for wideband Wilkinson power dividers do not exist. The existing MATLAB scripts that were used for the Bagley power dividers was modified for calculating the impedances of each section, as well as the resistors in between each section. The resulting dimensions for a wideband Wilkinson power divider operating between 0.7 and 3.5GHz is shown in the table below.

Table 11. Calculated Values for Wideband WPD.

Line	Z (Ω)	W (mm)	L (mm)
o	50.000	1.819	10
1	87.860	0.628	19.900
2	75.347	0.875	20.000
3	63.698	1.206	19.900
4	54.640	1.573	20.000
R1	120.000	1.250	2.000
R2	222.000	1.250	2.000
R3	294.000	1.250	2.000
R4	400.000	1.250	2.000

The simulated results are plotted below.

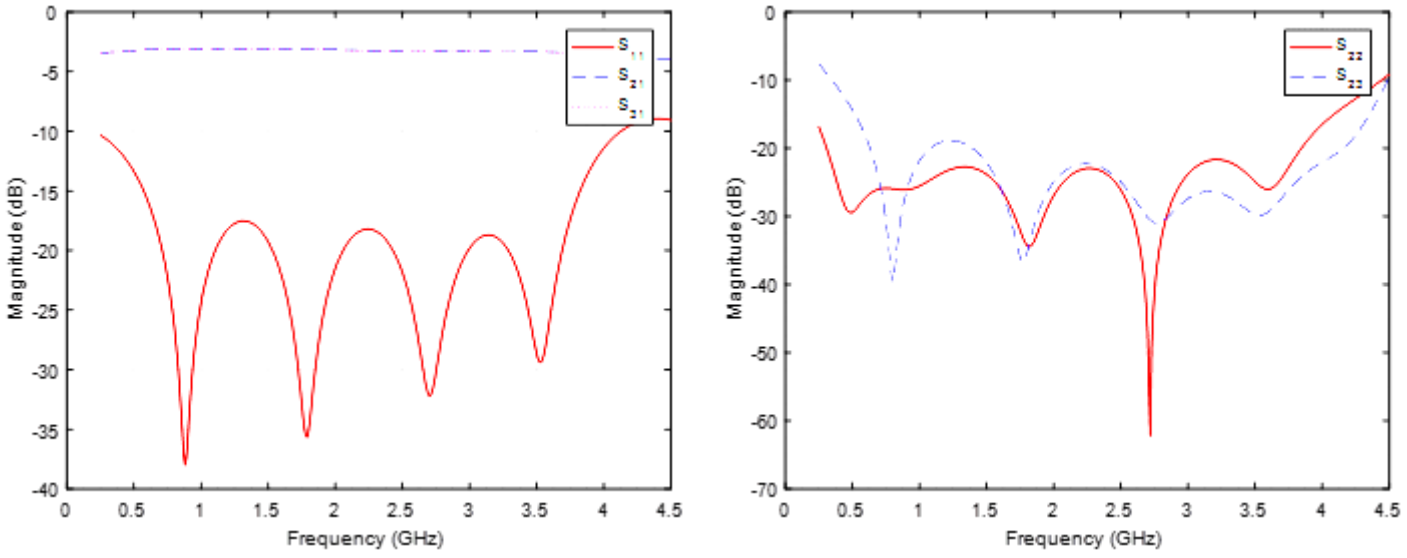

(a) (b)

Figure 24. S-Parameters of Wideband WPD (a) Input Port Matching and Transmission and (b) Output Port Matching and Isolation at 0.7-3.5 GHz.

Unequal Split Dual-Band Wilkinson Power Divider:

By utilizing both multi-section transmission lines and T-section structures with open stubs, a dual-band Wilkinson power divider with a 1:5 power division ratio was designed. With unequal power division, ⅙ of the power is transmitted through one output port and ⅚ of the power is transmitted through the other.

First, the conventional unequal-split Wilkinson power divider was examined, as shown by the following figure:

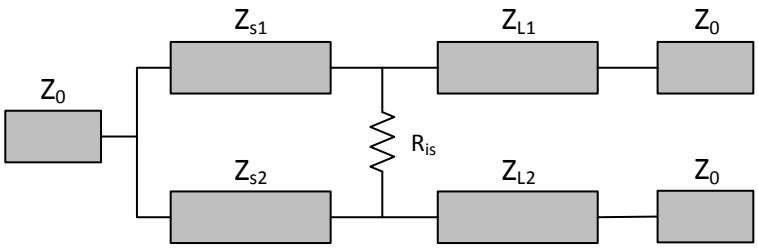

Figure 25. Schematic Diagram of an Unequal Split WPD.

The impedances of each section are calculated by the equations below [1].

$$Z_{S1} = Z_0\left(1+\frac{1}{K^2}\right)$$

$$Z_{L1} = \frac{Z_0}{K}$$

$$Z_{S2} = Z_0\left(1+K^2\right)$$

$$Z_{L2} = KZ_0$$

In an unequal split power divider, the ratio is expressed by $1:K^2$. In this case, a 1:5 split was designed, so K^2 is equal to 5. The characteristic impedance of the top branch and bottom branch is calculated by:

$$Z_{M1} = \sqrt{Z_{S1}Z_{L1}}$$

$$Z_{M2} = \sqrt{Z_{S2}Z_{L2}}$$

In the design of a 1:5 split, the impedance of Z_{M2} was 183.14 Ω, resulting in a transmission line width of 0.056 millimeters which was too small for a circuit board milling machine to fabricate. The solution to this problem was to introduce T-section structures. The idea was to replace the problematic high-impedance line with two equivalent T-section structures in which each structure is comprised of two transmission lines and an open stub in between. A diagram of the structures is shown in the figure below.

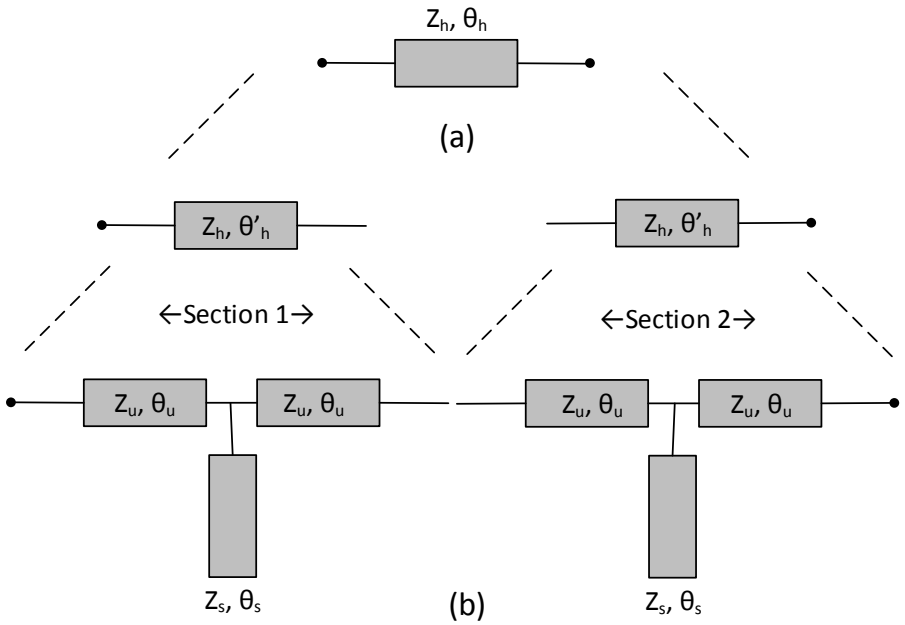

Figure 26. Schematic Diagram of (a) The High Impedance Line and (b) the Equivalent Dual-Band T-Section Structures.

Z_u is the impedance of the transmission lines, Z_S is the impedance of the stub, and θ_u and θ_s are the electrical lengths. The equations used to calculate the values are as follows:

First the ratio of the frequencies is defined as

$$R_f = \frac{f_2}{f_1}$$

Which in this case f_1=0.7 and f_2=1.7. The electrical length of the *u*-section is

$$\theta_u = \frac{\pi}{1+R_f}$$

And the impedance of the *u*-section is

$$Z_u = Z_h \frac{\cot(\theta_u)\sin(\theta_h')}{1+\cos(\theta_h')}$$

Where θ_h' is equivalent to 45° because the high impedance line is split into two sections, and Z_h is the high impedance line which in this case is 183.14 Ω. The electrical length of the stub, θ_s, is defined as $2\theta_u$ and used for determining the impedance of the stub by

$$Z_S = \frac{1}{2} Z_u \frac{\tan(\theta_S)\sin(\theta_S)}{\cos(\theta_S) - \cos(\theta_h')}$$

The matching circuit for the high impedance line used the same technique, and the low impedance line utilized Monzon's theory of dual-band operation which was explored in the section on dual-band Bagley power dividers. The complete circuit is displayed in the figure below.

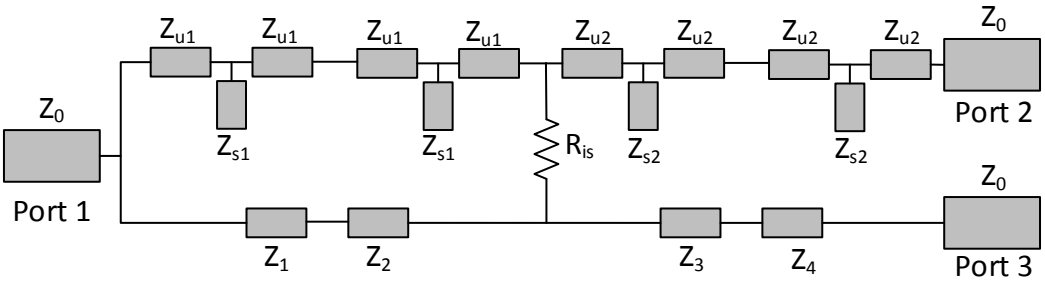

Figure 27. Schematic Diagram of the Dual-Band Unequal Split WPD.

The isolation resistor is calculated by [1]:

$$R_{is} = \frac{Z_0\left(K^2 + 1\right)}{K}$$

The impedances and corresponding lengths and widths of the transmission lines for the circuit are shown in the table below.

Table 12. Calculated Values for Dual-Band Unequal Split WPD.

Line	Z (Ω)	W (mm)	L (mm)
U1	58.200	1.414	37.836
S1	108.620	0.369	78.770
Z1	40.388	2.520	36.794
Z2	33.218	3.320	36.794
U2	23.764	5.158	35.940
S2	44.344	2.193	74.420
Z3	30.845	3.675	36.603
Z4	36.246	2.944	36.603
Ris	134	1.250	2.000

The simulated results from HFSS are plotted below. The simulated input/output port matching and isolations at both design frequencies are less than -20 dB; where as S_{21} and S_{31} are close to their theoretical values of -7.78 dB and -0.8 dB with ±0.5 dB tolerance.

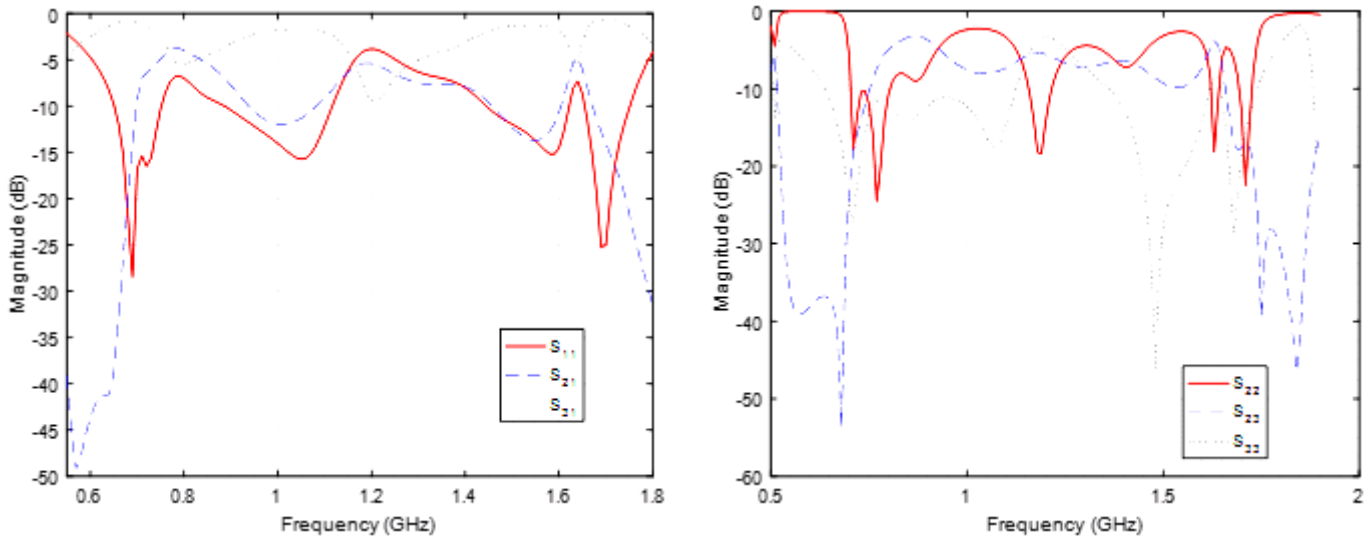

Figure 28. S-Parameters of Unequal Split Dual-Band WPD (a) Input Port Matching and Transmission and (b) Output Port Matching and Isolation at 0.7 and 1.7 GHz.

Square Patch Antennas

Description: Microstrip antennas were designed using parametric analysis and their radiation patterns and gain were simulated. The same RO4003C substrate was used, and similar operating frequencies were chosen. The antennas were designed to be directional, meaning that they transmit and receive electromagnetic waves from only one direction.

This stage was divided into two activities.

Single-Band Square Patch Antennas:

Single-band antennas that can be printed directly onto a circuit board were designed. A model of the antenna is shown in the figure below.

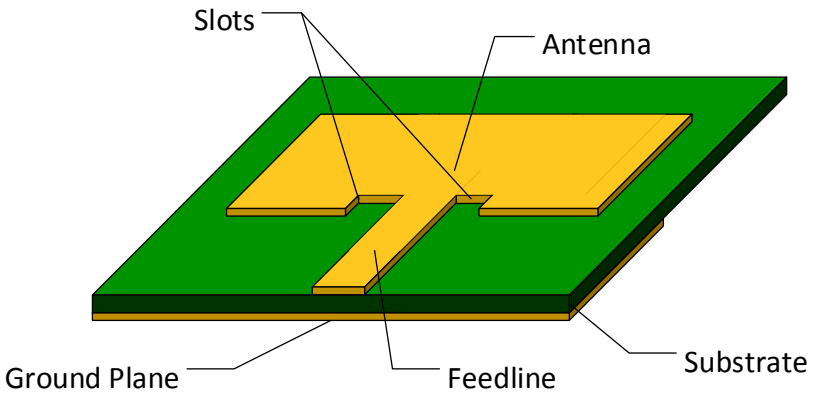

Figure 29. Square Patch Antenna Built on a Substrate.

Because of their low cost and ease of fabrication, several calculators exist for determining the size of the patch antenna for a given frequency.

$$Width = \frac{c}{2 f_0 \sqrt{\frac{\varepsilon_r + 1}{2}}}$$

$$Length = \frac{c}{2 f_0 \sqrt{\varepsilon_{eff}}} - 0.824h \left(\frac{\left(\varepsilon_{eff} + 0.3\right)\left(\frac{W}{h} + 0.264\right)}{\left(\varepsilon_{eff} - 0.258\right)\left(\frac{W}{h} + 0.8\right)} \right)$$

However, further optimizations were done using parametric analysis in HFSS. Parametric analysis involves specifying a range of parameters, such as the length and width of the square patch, the feed line, or the slots, and simulating each case. The resulting plots reveals the best performing dimensions. For an antenna operating on 2.1 GHz, the parametric analysis that varied the width of the antenna, the length of the feedline, and the width and length of the slots resulted in the following plot:

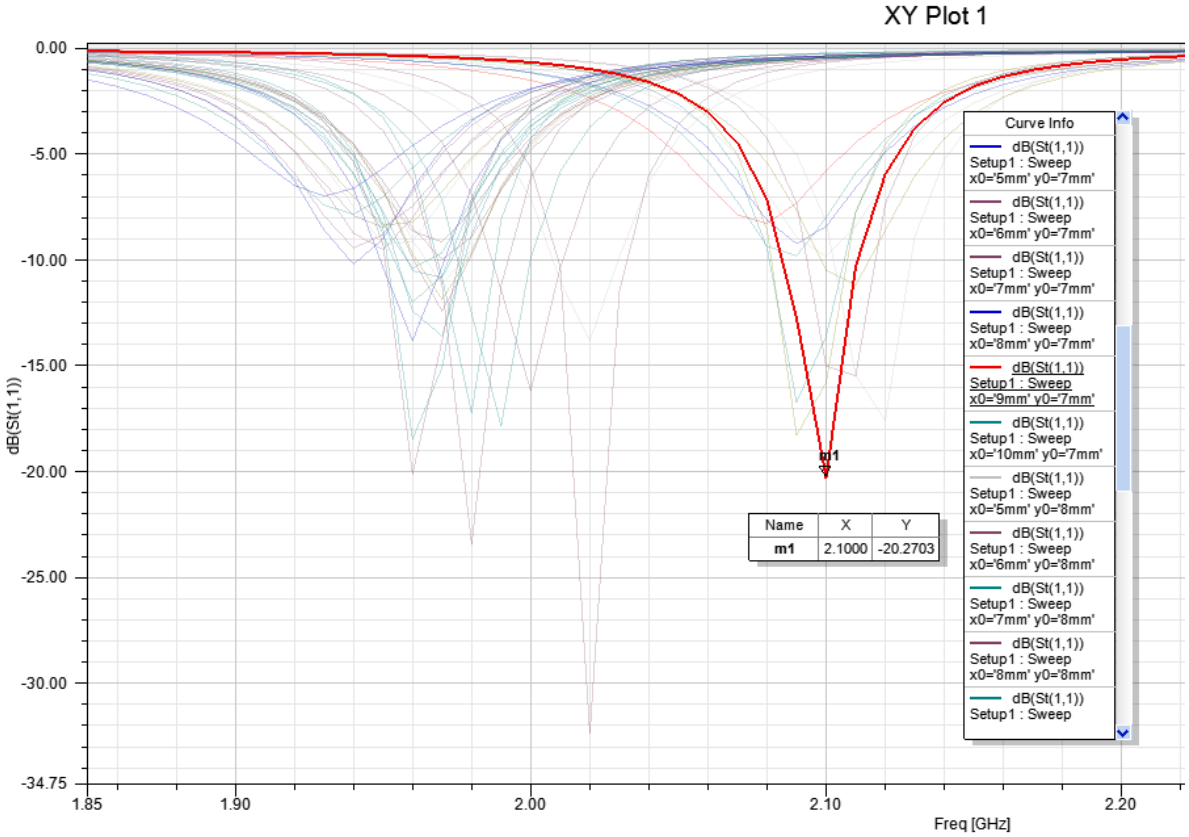

Figure 30. HFSS Antenna Parametric Analysis.

Based on the plot, the highlighted line was chosen for its good performance at 2.1 GHz. The required dimensions are shown in the figure below, and a table of the dimensions for the antenna are shown in the table below.

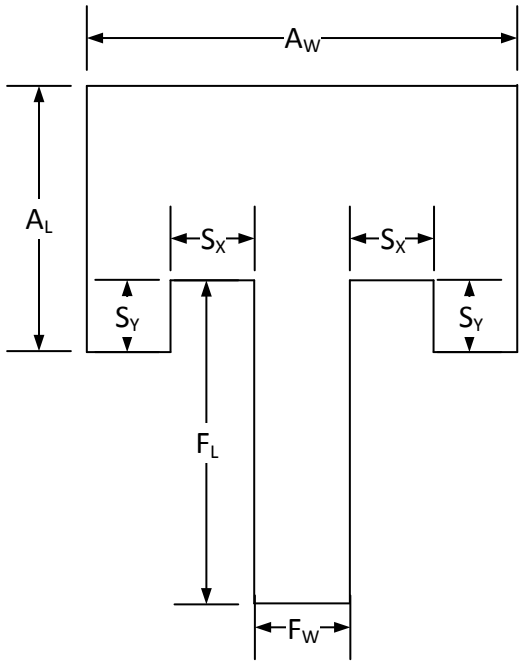

Figure 31. Dimensions of a Square Patch Antenna.

Table 13. Parametric Analysis Resulting Dimensions of a Square Patch Antenna for 2.1 GHz.

A_W (mm)	A_L (mm)	F_W (mm)	F_L (mm)	S_X (mm)	S_Y (mm)
47.320	37.730	1.819	5.000	9.000	7.000

Once the final dimensions were known, the antenna was simulated in HFSS. First, the S-parameters were plotted, as shown by the following plot:

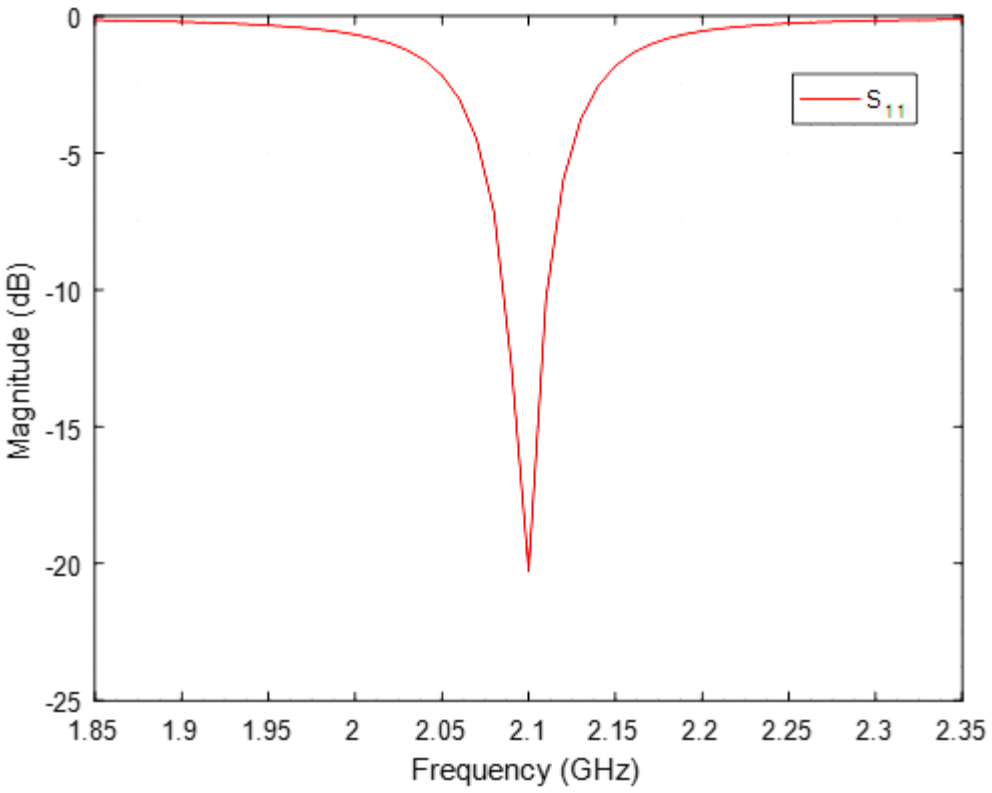

Figure 32. S-Parameters of Square Patch Antenna at 2.1 GHz.

Then the radiation pattern and gain were plotted:

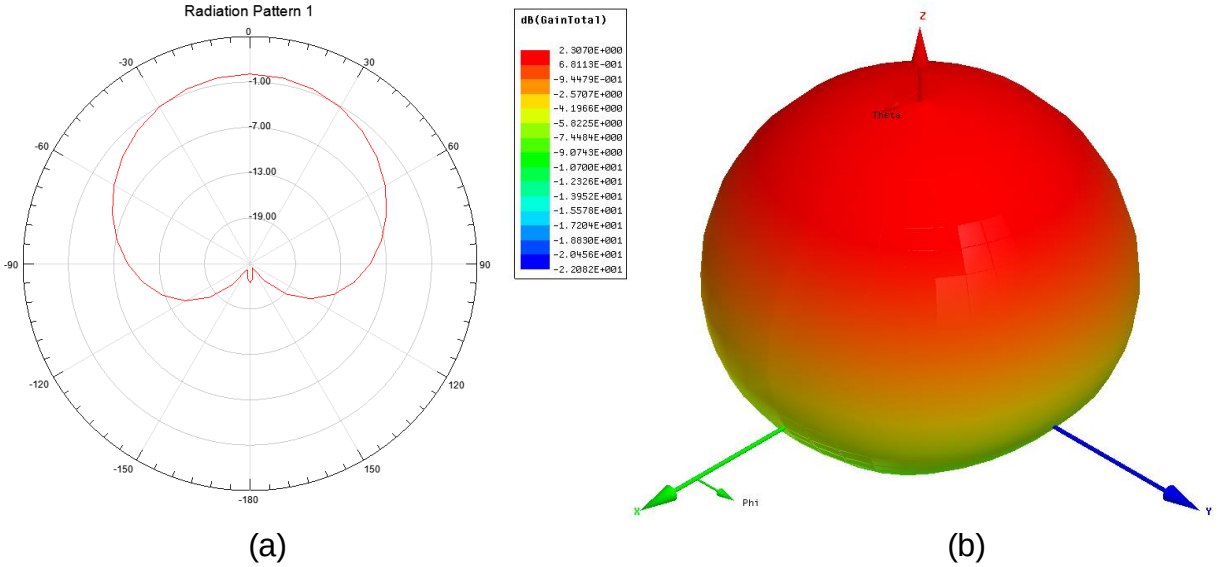

(a) (b)

Figure 33. Single-Band Square Patch Antenna (a) Radiation Pattern and (b) Gain, at 2.1 GHz.

In Figure 33, the antenna radiates outwards in one direction, confirming it operates as a directional antenna.

Dual-Band Square Patch Antennas:

The design of the single-band antenna was extended for dual-band operation by introducing two more slots on the antenna [7]. The dual-band antenna was designed for operating frequencies of 2.1 and 3.6 GHz.

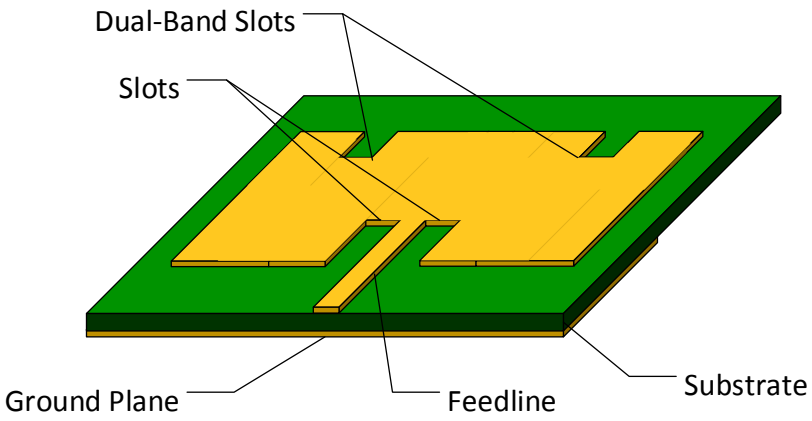

Figure 34. Dual-Band Square Patch Antenna Built on a Substrate.

Once again, a parametric analysis of the dimensions was performed in HFSS because standardized equations do not exist for this kind of antenna functionality. Initially, the dimensions of the dual-band slots were chosen to be symmetrical. Dual-band functionality was achieved, but not at the correct frequencies. By making the dimensions asymmetrical from each other, the proper frequencies were obtained within a reasonable margin.

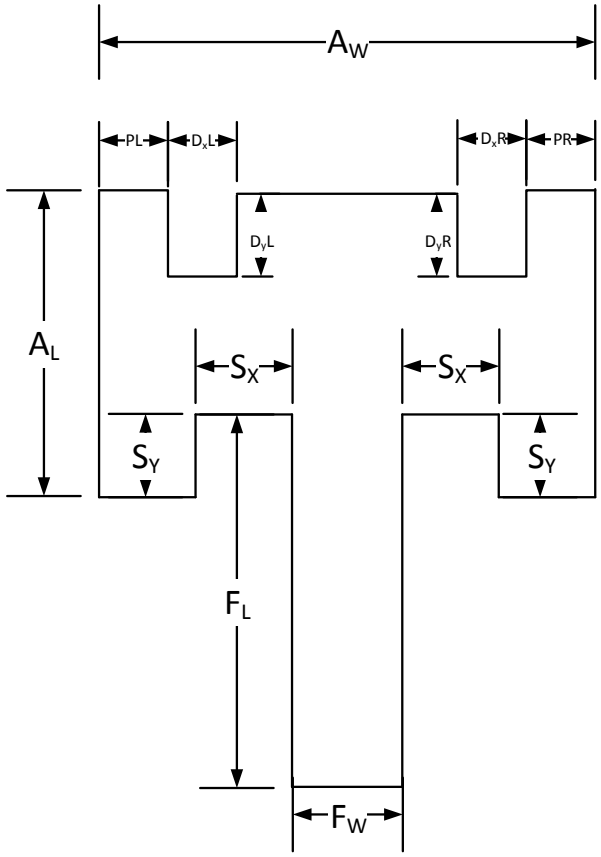

Figure 35. Dimensions of Dual-Band Square Patch Antenna.

Table 14. Parametric Analysis Resulting Dimensions of Dual-Band Square Patch Antenna for 2.1 and 3.6 GHz.

A_W	A_L	F_W	F_L	S_X	S_Y	PL	PR	DxL	DxR	DyL	DyR
47.320	37.730	1.819	5.000	14.000	2.200	4.500	0.800	11.000	8.000	3.000	3.500

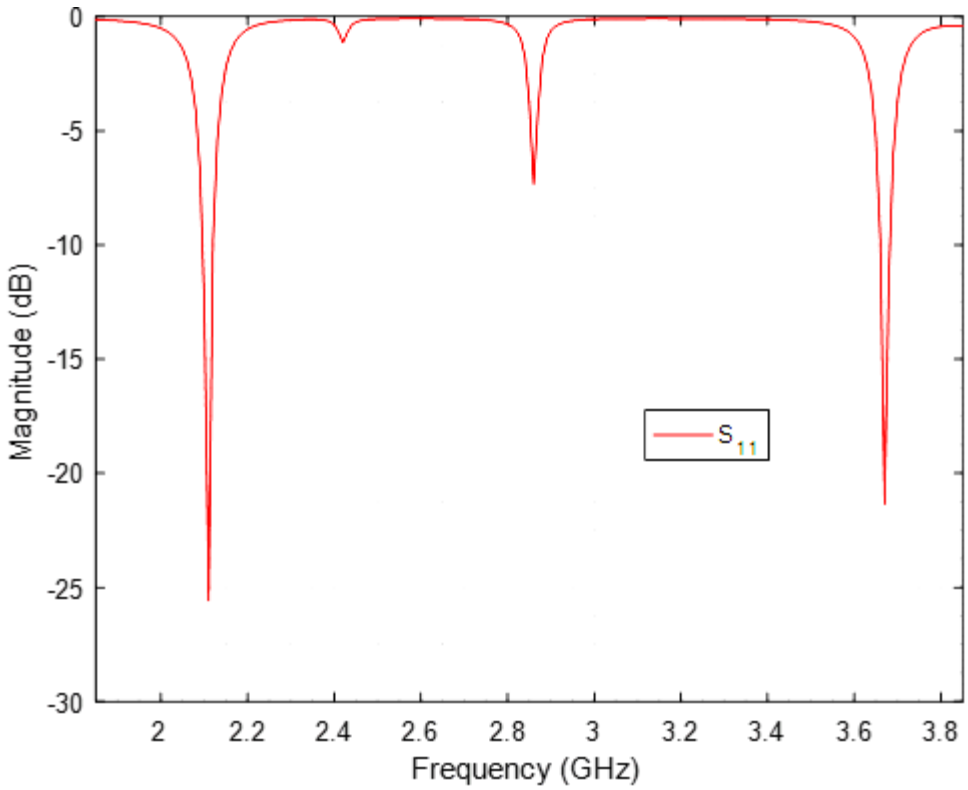

Figure 36. S-Parameters of Dual-Band Square Patch Antenna at 2.1 and 3.6 GHz.

The scattering parameters of the dual-band antenna confirm that it worked on the designated frequencies, but to confirm its directional performance the radiation pattern and gain of the antenna must be simulated on 2.1 GHz and 3.6 GHz separately.

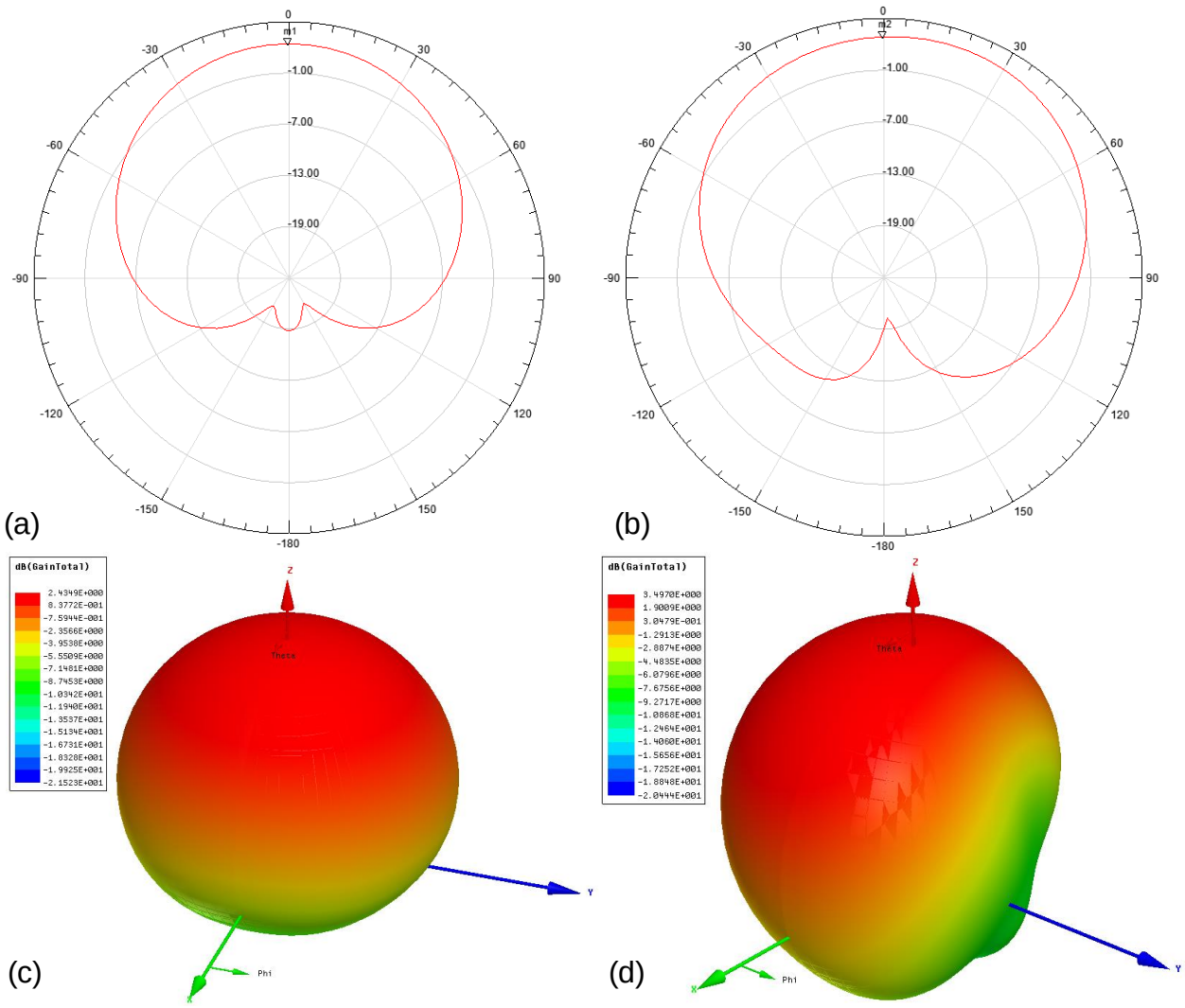

Figure 37. 2D Radiation pattern at (a) 2.1 GHz and (b) 3.6 GHz, and 3D Radiation Patterns at (a) 2.1 GHz and (b) 3.6 GHz.

It is important to note that the radiation pattern of the antenna operating 3.6 GHz was fine-tuned by performing parametric analyses that resulted in slightly different dimensions.

Fabrication and Measurements

Description: The design team traveled to the University of Akron, in Akron, Ohio for fabrication and measurement of the miniaturized quad-band Bagley power divider, the wideband Wilkinson power divider, and the 1:5 dual-band Wilkinson power divider. The design team met with Dr. Arjuna Madanayake and two of his Ph.D. students, Sravan Pulipati and Viduneth Arlyarathna, who helped with operating the milling machine and the network analyzer.

This stage was divided into two activities.

Fabrication:

Fabrication was done using a LPKF ProtoMat S103 milling machine. Three designs, the miniaturized quad-band Bagley power divider, the four-section wideband Wilkinson power divider, and the dual-band 1:5 unequal split Wilkinson power divider, were chosen to be fabricated. First, the HFSS files were converted to a *.sab* file format, and then opened in CST Microwave Studio and converted to a *.gbr* file format which is accepted by the milling machine. The files were loaded into the milling machine software and the types of drills and tools were selected to be used. The substrate was taped down in the machine and correctly aligned.

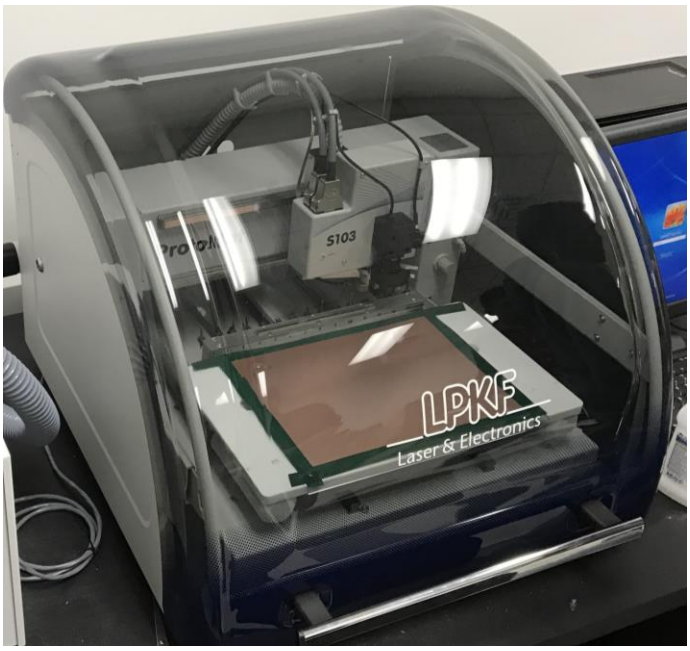

Figure 38. LPKF ProtoMat S103 PCB Milling Machine.

Once everything was ready, the machine started its fully automated process. The machine grounded off the unwanted copper, leaving the conductive traces.

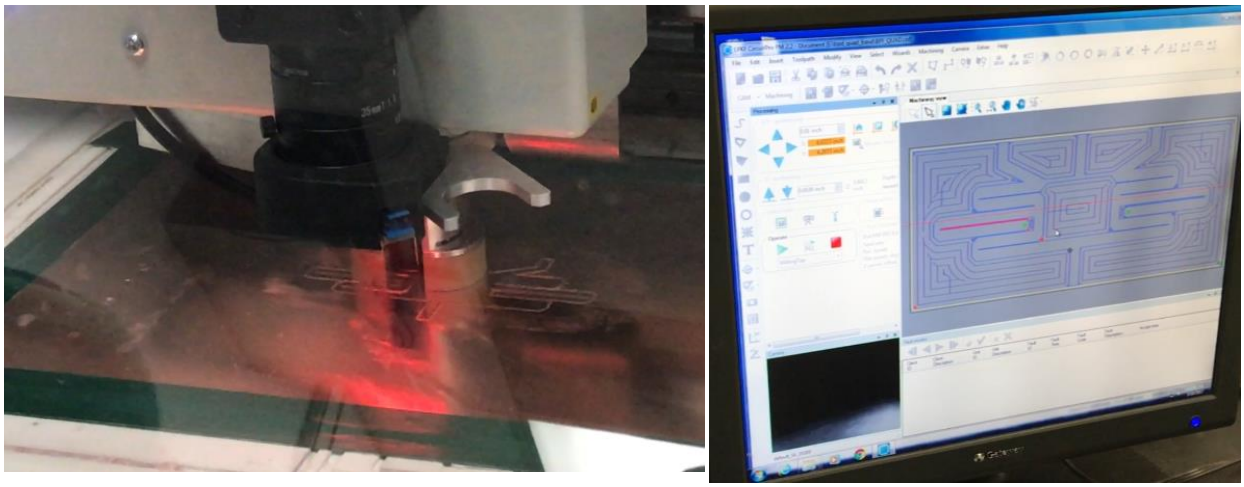

(a) (b)

Figure 39. LPKF Milling Machine (a) In Action and (b) Software.

The completed circuit was cut out from the substrate, and the SMA connectors and resistors were soldered on.

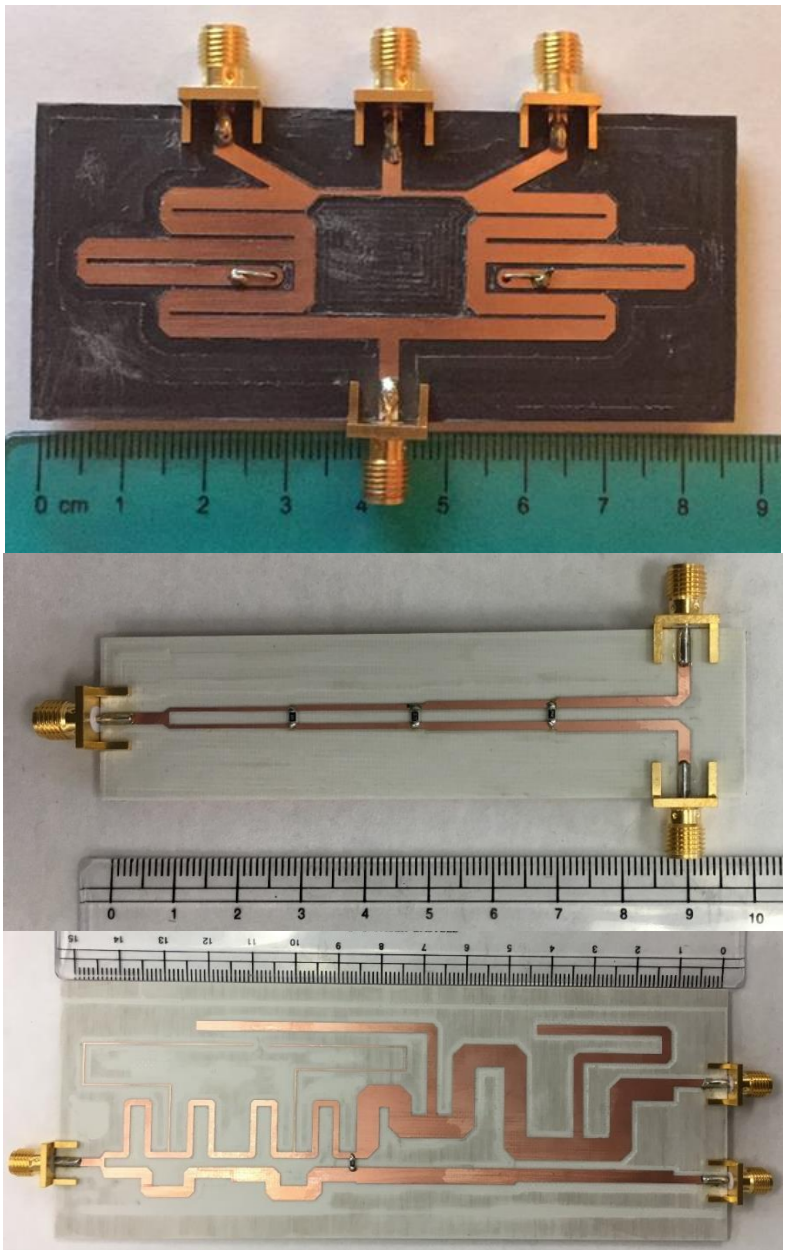

Figure 40. Fabricated Components. Top: Quad-Band BPD Using Coupled Lines, Middle: Wideband WPD, Bottom: Dual-Band Unequal Split WPD.

Measurements:

Measurements of the fabricated components were done using an Agilent Technologies E5071C vector network analyzer.

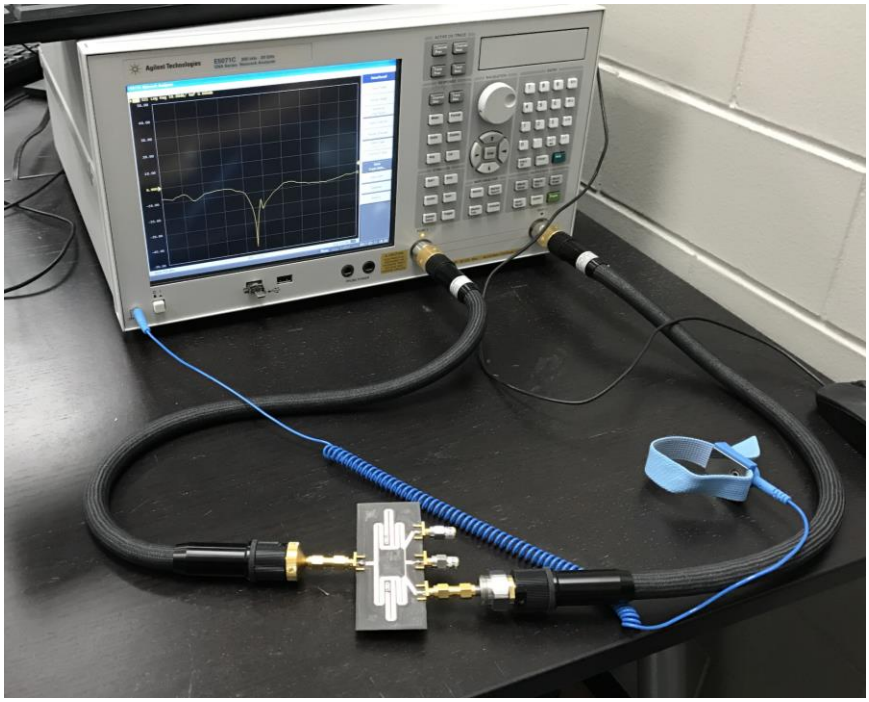

Figure 41. Network Analyzer Setup

The network analyzer measures the S-parameters of one output port at a time, so matched loads are attached to the other output ports. The data was saved and comparisons between the simulated and measured components are shown in the plots below.

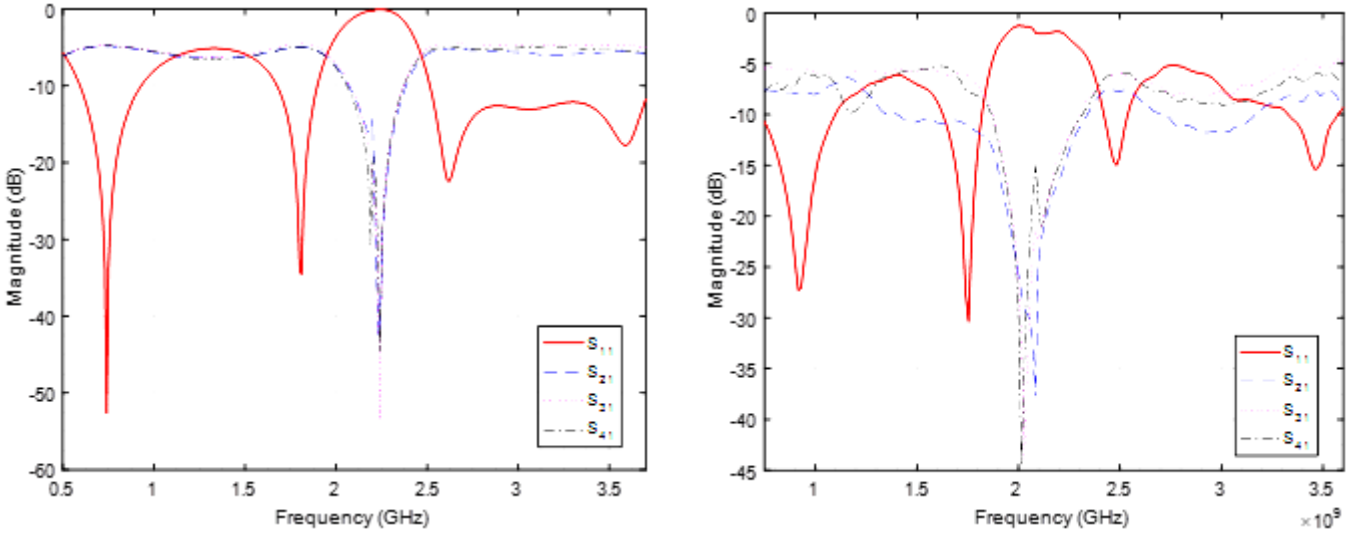

Figure 42. S-Parameters of Quad-Band BPD Using Coupled Lines (a) Simulated Results and (b) Measured Results.

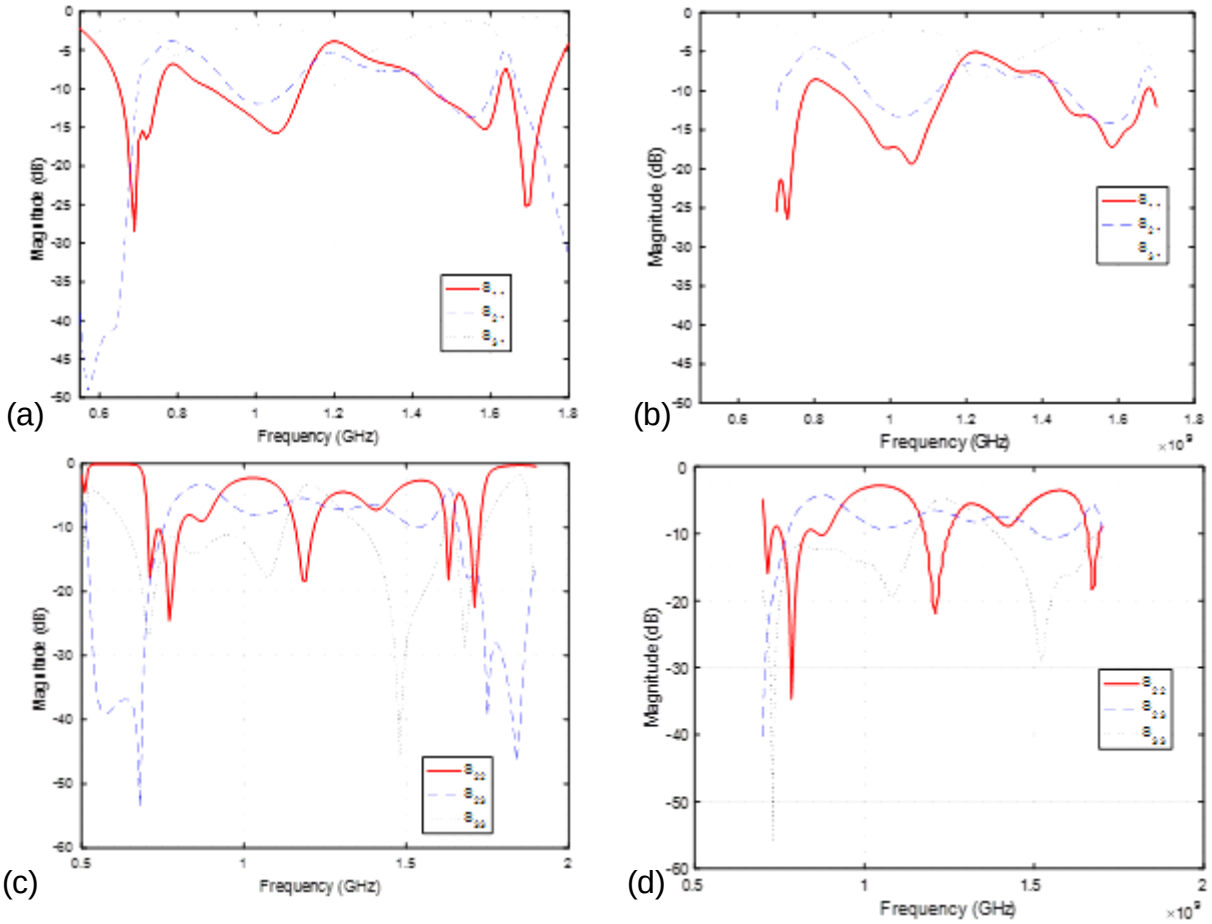

Figure 43. S-Parameters of Dual-Band Unequal Split WPD (a) Simulated Input Port Matching / Transmission (b) Measured Input Port Matching and Transmission (c) Simulated Output Port Matching and Isolation (d) Measured Output Port Matching and Isolation.

Due to a calibration error and time constraints, proper measurements of the wideband Wilkinson power divider were not obtained.

Conclusions

In this project the senior design team researched and designed power dividers, power couplers, and antennas. Using advanced simulation tools and other various types of software, the designs were simulated for peak optimization. Once this was achieved, a handful of final designs were fabricated. Fabrication and measurement took place at Akron University in Ohio. The objectives of designing improved microstrip components was achieved, as well as publishing at least one paper during this project.

The components that were researched and designed in this project are only a small portion of what could be done given more time and resources. Future design teams can use this work as a guideline for their own designs of similar components, or use these designs in a larger project such as an amplifier circuit.

References

1. D. Pozar. *Microwave Engineering*. 4th ed. Hoboken, NJ: Wiley. 2012.
2. I. Sakagami, T. Wuren, M. Fujii, and M. Tahara. “Compact Multi-Way Power Dividers Similar to the Bagley Polygon.” University of Toyama, Department of Electrical and Electronics Engineering. 2007.
3. C. Feng, G. Zhao, X.-F. Liu and F.-S. Zhang, "A Novel Dual-Frequency Unequal Wilkinson Power Divder," *Microwave and Optical Technology Letters,* vol. 50, no. 6, pp. 1695-1699. 2008.
4. M. Almalkawi, K. Al Shamaileh, S. Abushamleh and H. Al-Rizzo, "A New Class of Compact Linear Printed Antennas," *Progress in Electromagnetics Research,* vol. 57, pp. 61-69. 2015.
5. X. Li, M. Helaoui, F. Ghannouchi, W. Chen, “A Quad-Band Doherty Power Amplifier Based on T-Section Coupled Lines,” *IEEE Microwave and Wireless Components Letters*, vol. 26, no. 6, pp. 437-439. 2016.
6. K. Shamaileh, M. Almalkawi, N. Dib, B. Henin, and A. Abbosh, “Fourier-Based Transmission Line Ultra-wideband Wilkinson Power Divider for EARS Applications,” in *IEEE International Midwest Symposium on Circuits and Systems*, Columbus, 2013.
7. S.K. Behera and Y. Choukiker, “Design and Optimization of Dual Band Microstrip Antenna Using Particle Swarm Optimization Technique,” *Journal of Infared, Millimeter, and Terahertz Waves*, pp. 1346-1354. 2010.

Acknowledgements

The design team and the advisor acknowledge Arjuna Madanayake, Associate professor at the University of Akron, and Sravan Pulipati, and Viduneth Arlyarathna, Ph.D. students at the University of Akron, for their assistance in providing means of fabrication and measurement facilities at the University of Akron.

Appendix A: Additional Simulated Results

Several more Bagley power dividers were designed and their simulated results can be found here.

Conventional:

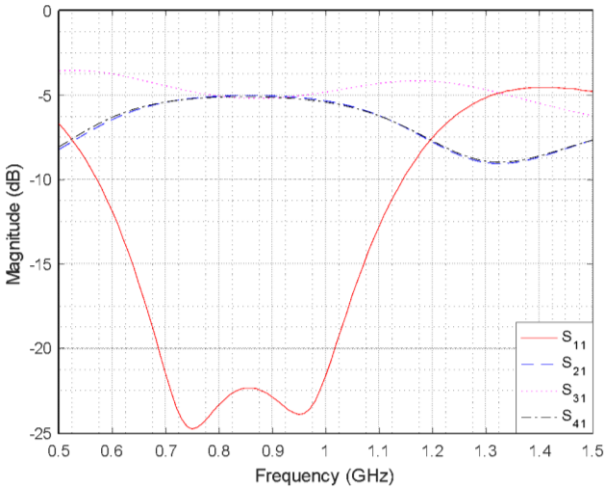

Result 1. Three-Way BPD at 0.870 GHz

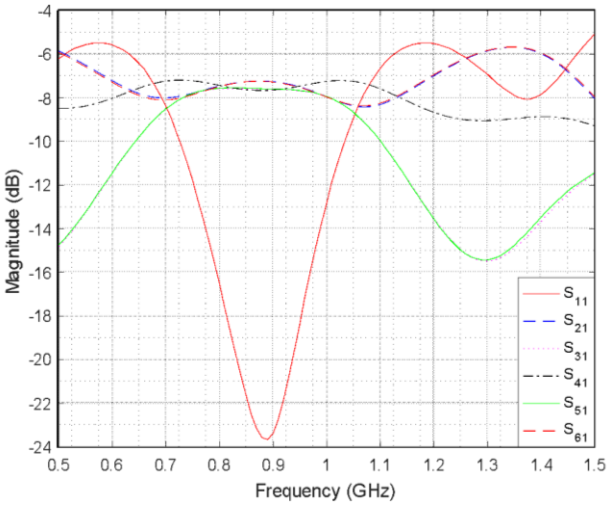

Result 2. Five-Way BPD at 0.870 GHz

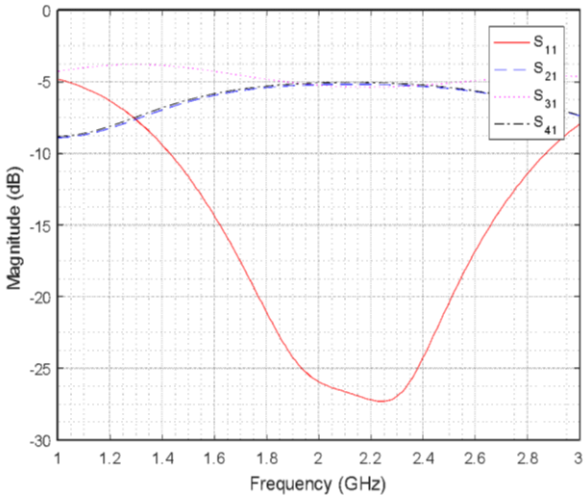

Result 3. Three-Way BPD at 2.13 GHz

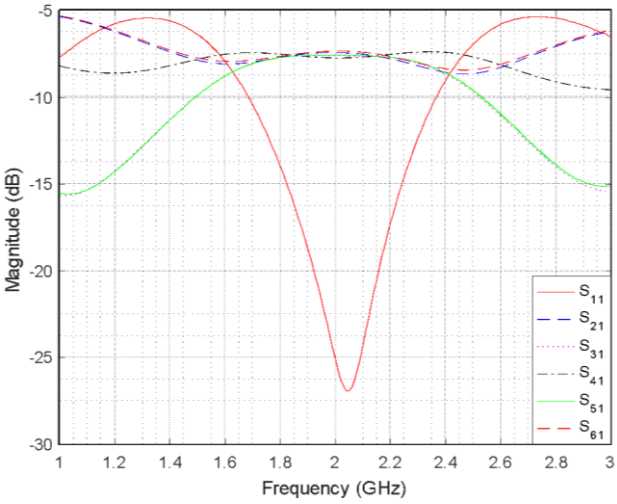

Result 4. Five-Way BPD at 2.13 GHz

Modified:

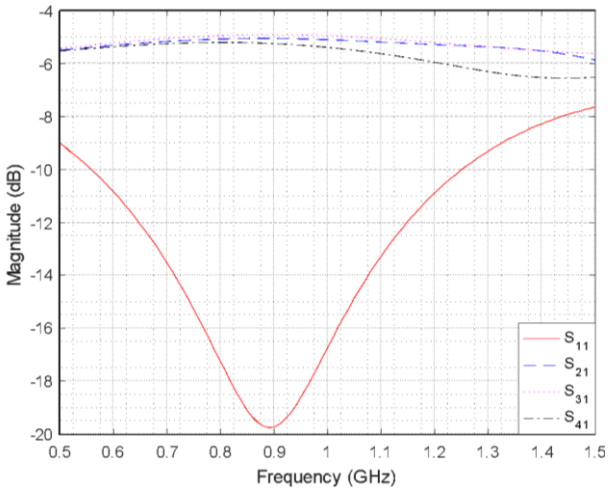

Result 5. Three-Way BPD at 0.870 GHz

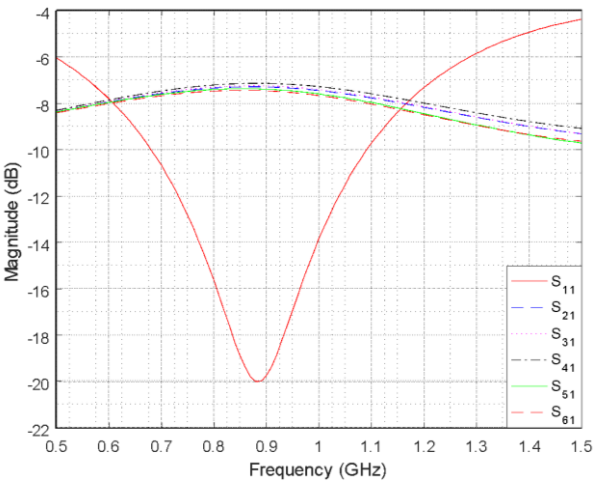

Result 6. Five-Way BPD at 0.870 GHz

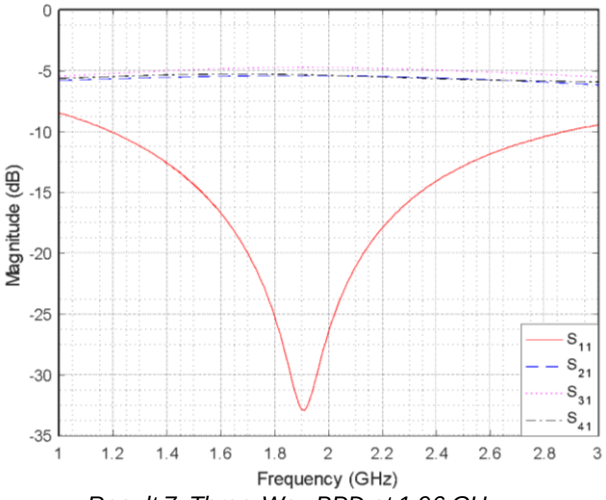

Result 7. Three-Way BPD at 1.96 GHz

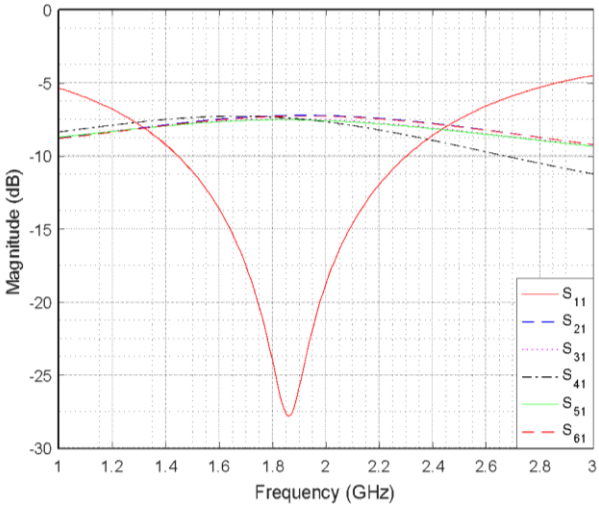

Result 8. Five-Way BPD at 1.96 GHz

Dual-Band:

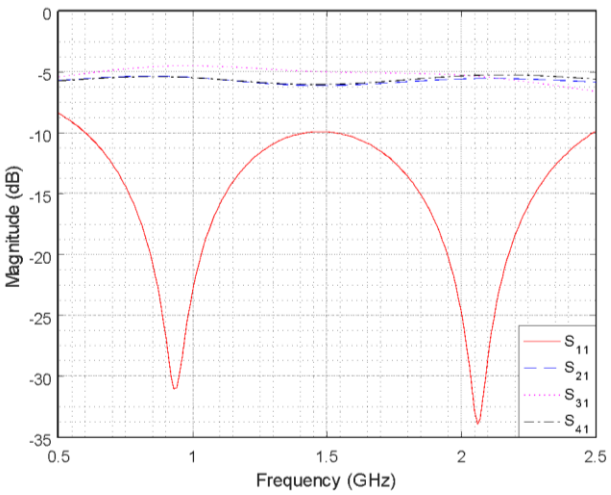

Result 9. Three-Way BPD at 0.870 and 1.96 GHz

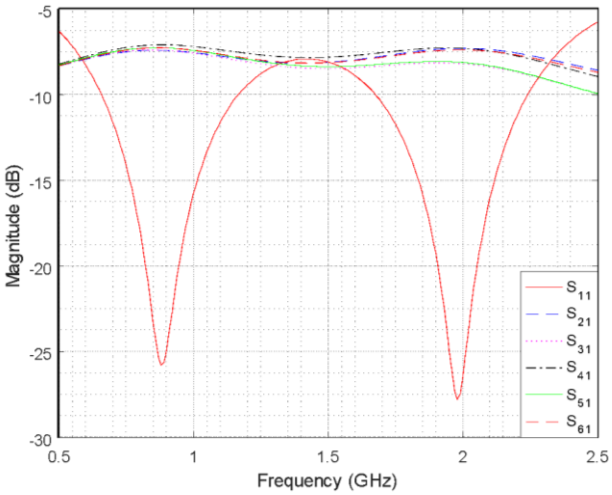

Result 10. Five-Way BPD at 0.870 and 1.96 GHz

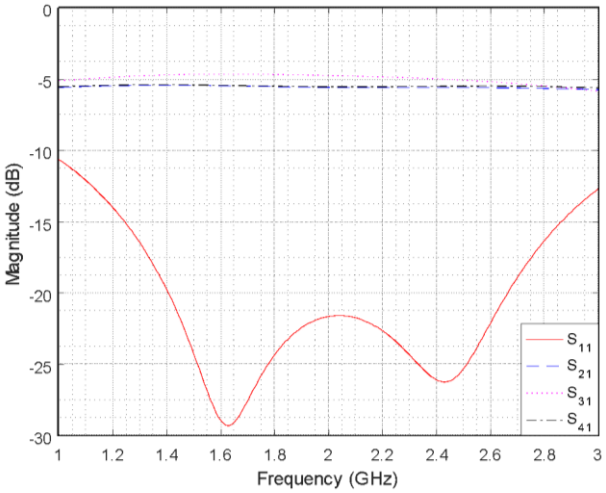

Result 11. Three-Way BPD at 1.96 and 2.13 GHz

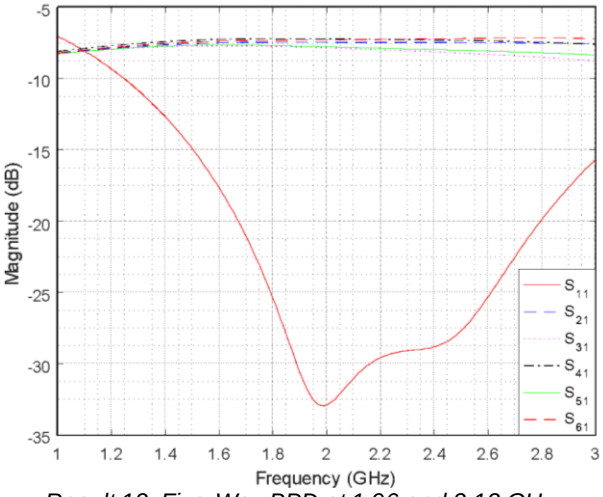

Result 12. Five-Way BPD at 1.96 and 2.13 GHz

Appendix B: Updated Work Plan

Milestone Log

Tasks	Target Date
1. Bagley Power Dividers	
a. Single-Band	10/21/16
b. Dual-Band	11/02/16
c. Tri-Band+Quad-Band	12/04/16
d. Miniaturized Quad-Band	01/15/17
2. Wilkinson Power Dividers and Couplers	
a. Single-Band	01/22/17
b. Wideband	02/12/17
c. Dual-Band Unequal Split	03/05/17
3. **Square Patch Antennas**	
a. Single-Band	04/05/17
b. Dual-Band	04/19/17
4. Fabrication and Measurements	
a. PCB Fabrication and Measurements	03/10/17

Appendix C: 2017 IEEE AP-S/URSI Conference Paper

Quad-band Multi-section Multi-way Power Divider and its Miniaturization Using Coupled Lines

Michael Knizek, Christopher Nicholl, Craig Popovich, Khair Al Shamaileh
Electrical and Computer Engineering Department
Purdue University Northwest
Hammond, USA
MikeKnizek23@gmail.com, ChrisJNicholl@gmail.com, Popovich.Craig@gmail.com, Kalshama@pnw.edu

***Abstract*—We propose a general guideline to design a three-way quad-band Bagley power divider (BPD) by replacing the quarter-wave transformer in the conventional design with multi-section transmission lines. A constrained nonlinear optimization process is performed based on transmission lines theory to obtain the optimal impedances and lengths of each section. We also propose a miniaturized quad-band BPD structure using coupled line transformers. Simulated results of both techniques show an input port matching less than –15 dB and transmission parameters of –4.77±0.5 dB at each frequency of operation.**

Keywords—Bagley power divider (BPD), coupled lines, multi-section transmission lines, quad-band.

INTRODUCTION

Power dividers are among various front-end components that are used in modern circuitry, such as voltage standards, feeding networks, power amplifiers and mixers [1, 2]. The Bagley power divider (BPD) is among various divider types, and is recently being used in filtering circuitry [3]. However, the conventional design of the BPD is limited to narrowband applications due to the incorporation of single-frequency matching quarter-wave transformers in its structure. Hence, various techniques were reported to further enhance the operating bandwidth of microstrip BPDs, such π-/T-networks [4]. However, the resulting multiband response was at the expense of an increase in physical area or fabrication complexity. In this paper, we propose a quad-band multi-section BPD based on transmission lines analysis. Then, a compact counterpart quad-band divider is designed and verified using coupled-line transformers.

MULTI-BAND BPD DESIGN

In this section, two methods to design a three-way quad-band BPD operating at 0.73, 1.65, 2.67 and 3.57 GHz are presented using: 1) multi-sectioning, and 2) coupled-lines.

Quad-band Multi-section BPD

Figure 1(a) shows a schematic diagram of the proposed multi-section quad-band BPD; whereas Fig. 1(b) shows the even-mode equivalent circuit. The incorporation of multi-section transmission lines enables the power divider to operate at multiple frequencies, four in this case. The multi-section lines have impedances denoted as $Z_{1,2,3,4}$. Since there are no exact formulas to obtain the impedances and lengths

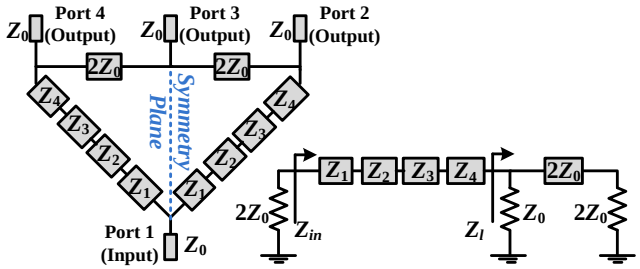

Fig. 1. Quad-band BPD: (a) schematic diagram, (b) even-mode circuit.

of a four-section line, an optimization process is performed. The *ABCD* matrix of a section with length l_i (i=1, 2, 3, 4) at frequency f_k (k=1, 2, 3, 4) can be given as:

$$\begin{bmatrix} A_{ik} & B_{ik} \\ C_{ik} & D_{ik} \end{bmatrix}_{Z_i} = \begin{bmatrix} \cos(\theta_{ik}) & jZ_i \sin(\theta_{ik}) \\ jZ_i^{-1} \sin(\theta_{ik}) & \cos(\theta_{ik}) \end{bmatrix} \quad (1)$$

where θ_{ik} is the electrical length of the i^{th} section given as:

$$\theta_{ik} = 2\pi\left(l_i f_k \sqrt{\varepsilon_{eff}}/c\right) \quad (2)$$

ε_{eff} is the effective dielectric constant, and c is the speed of light. The *ABCD* matrix of the four-section line at f_k is found by multiplying the *ABCD* matrix of each section as follows:

$$ABCD_k = \begin{bmatrix} A_{1k} & B_{1k} \\ C_{1k} & D_{1k} \end{bmatrix} \cdot \begin{bmatrix} A_{2k} & B_{2k} \\ C_{2k} & D_{2k} \end{bmatrix} \cdot \begin{bmatrix} A_{3k} & B_{3k} \\ C_{3k} & D_{3k} \end{bmatrix} \cdot \begin{bmatrix} A_{4k} & B_{4k} \\ C_{4k} & D_{4k} \end{bmatrix} \quad (3)$$

The input impedance, Z_{in}, shown in Fig. 1(a) at f_k can be calculated using the following expression:

$$Z_{in}(f_k) = \frac{ABCD_k(1,1)\cdot Z_l + ABCD_k(1,2)\cdot Z_l}{ABCD_k(2,1)\cdot Z_l + ABCD_k(2,2)\cdot Z_l} \quad (4)$$

where $Z_l = Z_0//2Z_0 = 2Z_0/3$. Upon determining Z_{in} at f_k, the input reflection coefficient, $\Gamma_{in}(f_k)$, can be given as:

$$\Gamma_{in}(f_k) = \left[Z_{in}(f_k) - 2Z_0\right] / \left[Z_{in}(f_k) + 2Z_0\right] \quad (5)$$

For a perfect input port matching at the design frequencies, Γ_{in} at f_k should be zero (or very small). Thus, the following error function is minimized considering $20\Omega \le Z_{1,2,3,4} \le 100\Omega$, $5\text{mm} \le l_{1,2,3,4} \le 30\text{mm}$, $Z_0 = 50\Omega$ port impedance, and 0.787mm thick RT5880 substrate with a relative permittivity of 2.2:

$$Error = \sum_{k=1}^{4} \left|\Gamma(f_k)\right|^2 \quad (6)$$

Table I shows the resulting optimized impedances and lengths of each section. Optimization is performed in 3000 iteration using "fmincon" subroutine in MATLAB.

TABLE I. OPTIMIZED IMPEDANCES AND LENGTHS OF THE PROPOSED 3-WAY QUAD-BAND BPD.

Impedance	Z_i (Ω)	W (mm)	l_i (mm)
Z_1	73.11	1.31	25.60
Z_2	62.87	1.70	26.00
Z_3	53.02	2.22	25.80
Z_4	45.50	2.79	25.00

Quad-band Coupled Lines BPD

Figure 2 shows the proposed three-way quad-band divider using the T-section coupled lines concept [5]. The characteristic impedances of the coupled lines $Z_{A,B}$ are:

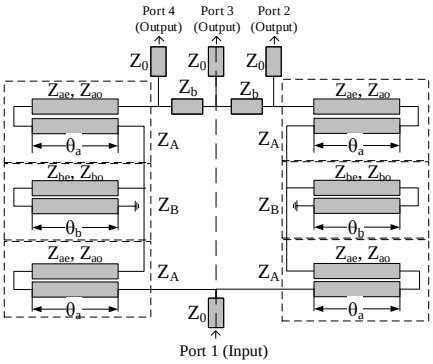

Fig. 2. Outline of three-way quad-band BPD using coupled lines.

$$Z_A = \sqrt{Z_{ae} \cdot Z_{ao}} \quad (7)$$

$$Z_B = \sqrt{Z_{be} \cdot Z_{bo}} \quad (8)$$

where $Z_{ae,ao}$ are the even- and odd-mode impedances of the coupled line Z_A; whereas $Z_{be,bo}$ are the even-mode and odd-mode impedances of the coupled line Z_B. Based to the analysis presented in [5], there are four solutions for the electrical length of each couple line: $\theta_{ak} = \theta_{bk} = \theta_k = \pi f_k / 2f_0$, where $f_0 = (f_1 + f_4)/2 = (f_2 + f_3)/2$. We utilize [5, eqns. (9)–(12)] to solve analytically for the even-odd mode impedances considering the characteristic impedance of the quarter-wave transformer, $Z_m = 2Z_0/\sqrt{3}$ in the conventional three-way BPD [4]. Once the even- and odd-mode impedances are known, widths, lengths, and separations can be found using the available microstrip coupled line calculators. Table II shows the electrical and physical characteristics of the proposed quad-band BPD. It is noteworthy to point out that the analytical values were fine-tuned to obtain the best simulated electrical performance at the design frequencies.

TABLE II. LINE IMPEDANCES, LENGTHS, WIDTHS AND SEPARATIONS FOR THE QUAD-BAND THREE-WAY BPD BASED ON COUPLED LINE SECTIONS.

Line	Z (Ω)	W (mm)	L (mm)	S (mm)
Z_{ae}	70.900	2.64	17.30	0.47
Z_{ao}	44.400			
Z_{be}	120.30	2.41	22.30	0.72
Z_{bo}	75.400			

RESULTS

Simulated results of the quad-band multi-section and T-section coupled lines BPDs are presented in Fig. 3(a) and Fig. 3(b), respectively. Input return loss better than 15 dB is obtained at the design frequencies for both dividers. Moreover, the transmission parameters are in the range of –4.77±0.5 dB, and are in close proximity to their theoretical values of –4.77 dB. Fig. 4 depicts a size comparison between both dividers. A size reduction of 62% is obtained in the case of adopting the T-section coupled lines technique as compared to multi-section transmission lines approach.

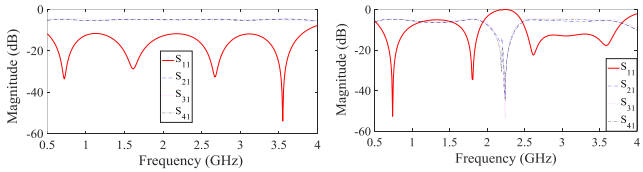

(a) (b)

Fig. 3. Simulated results of the quad-band three-way BPD using: (a) multi-section and (b) T-section coupled-line microstrip transmission lines.

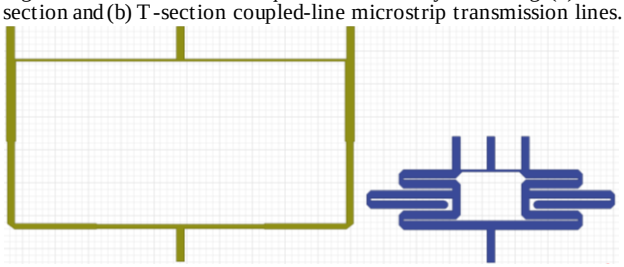

Fig. 4. Layouts of the multi-section and T-section coupled line BPDs.

CONCLUSION

In this paper, we proposed a quad-band three-way BPD using two design approaches. The first approach depends on replacing the quarter-wave transformer in the conventional design with a four-section transmission line. The impedances and lengths of each section are optimized to achieve the optimum input port matching at the design bands. The second approach adopts the concept of T-section coupled lines; where the various widths, lengths and separations are obtained analytically with the aid of the design equations presented in [5]. Simulated results justify the design approaches presented herein.

REFERENCES

M. Elsbury, P. Dresselhaus, N. Bergren, C. Burroughs, S. Benz, and Z. Popovic, "Broadband lumped-element integrated N-way power dividers for voltage standards," *IEEE Trans. Microw. Theory Techn.*, vol. 57, no. 8, pp. 2055–2063, 2009.

P.-H. Deng, and Y.-T. Chen, "New Wilkinson power dividers and their integration applications to four-way and filtering dividers," *IEEE Trans. Compon., Pack. Manuf. Technol.*, vol. 4, no. 11, pp. 1828–1837, 2014.

R. Garcia and M. Renedo, "Microwave single/multi-band planar filters with Bagley-polygon-type four-port power dividers," *IEEE MTT-S Int. Microw. Symp.*, 2012, Montreal, Canada, pp. 1–3.

A. Qaroot, K. Shamaileh, and N. Dib, "Design and analysis of dual-frequency modified 3-way Bagley power dividers," *Prog. Electromagn. Res. C*, vol. 20, pp. 67–81, Mar. 2011.

X. Li, M. Helaoui, F. Ghannouchi, and W. Chen, "A quad-band doherty power amplifier based on T-section coupled lines," *IEEE Microw. Wireless Compon. Letters*, vol. 26, no. 6, pp. 437–439, 2016.

Appendix D: Tri-Band MATLAB Code

```
function [Error_Fcn]=Tri_Band_Transformer(x)
% %% The substrate parameters:
E_r = 2.2;    h = 0.787e-3;     c = 3*10^8;
%
% %% THE DESIGN FREQUENCIES
 f1 = 0.73e9;
 f2 = 1.65e9;
 f3 = 2.67e9;


% Uniform Transmission Line Parameters (Optimization Variables)
l1 = x(1);        Z1 = x(4);
l2 = x(2);        Z2 = x(5);
l3 = x(3);        Z3 = x(6);

% Predefined Variables for the Bagley Power Divider
Z0 = 50;                              % Characteristic Impedance
N  = 3 ;                              % # of Output Ports
Zs = 2 * Z0;      Zl = (2 / N) * Z0;  % Source and Load Impedances

% ABCD Parameters of Z1 @ f1, f2, and f3
Aw1 = (Z1/60)*sqrt((E_r+1)/2)+((E_r-1)/(E_r+1))*(0.23+0.11/E_r);
Bw1 = (377*pi)/(2*Z1*sqrt(E_r));
Wid1=(8*exp(Aw1)*h)/(exp(2*Aw1)-2);

if Wid1>0 & Wid1<(2*h);
   W1 = Wid1;
else
   W1 = (2*h/pi)*(Bw1-1-log(2*Bw1-1)+((E_r-1)/(2*E_r))*(log(Bw1-1)+0.39-0.61/E_r));
end

% The value of the effective permettivity at each section:
E_eff1 = (E_r+1)/2+((E_r-1)/2)*(1/sqrt(1+12*h/W1));

% The normalized ABCD parameters @ f1
A1f1 = cos(2*pi*(l1)*f1*sqrt(E_eff1)/(c));
D1f1 = cos(2*pi*(l1)*f1*sqrt(E_eff1)/(c));
B1f1 = 1i*(Z1)*sin(2*pi*(l1)*f1*sqrt(E_eff1)/(c));
C1f1 = 1i*((Z1)^-1)*sin(2*pi*(l1)*f1*sqrt(E_eff1)/(c));

% The normalized ABCD parameters @ f2
A1f2 = cos(2*pi*(l1)*f2*sqrt(E_eff1)/(c));
D1f2 = cos(2*pi*(l1)*f2*sqrt(E_eff1)/(c));
B1f2 = 1i*(Z1)*sin(2*pi*(l1)*f2*sqrt(E_eff1)/(c));
C1f2 = 1i*((Z1)^-1)*sin(2*pi*(l1)*f2*sqrt(E_eff1)/(c));

% The normalized ABCD parameters @ f3
A1f3 = cos(2*pi*(l1)*f3*sqrt(E_eff1)/(c));
D1f3 = cos(2*pi*(l1)*f3*sqrt(E_eff1)/(c));
B1f3 = 1i*(Z1)*sin(2*pi*(l1)*f3*sqrt(E_eff1)/(c));
```

```
C1f3 = 1i*((Z1)^-1)*sin(2*pi*(l1)*f3*sqrt(E_eff1)/(c));

ABCD_1f1=[A1f1 B1f1;C1f1 D1f1]; ABCD_1f2=[A1f2 B1f2;C1f2 D1f2];
ABCD_1f3=[A1f3 B1f3;C1f3 D1f3];
```

ABCD Parameters of Z2 @ f1, f2, and f3

```
Aw2 = (Z2/60)*sqrt((E_r+1)/2)+((E_r-1)/(E_r+1))*(0.23+0.11/E_r);
Bw2 = (377*pi)/(2*Z2*sqrt(E_r));
Wid2=(8*exp(Aw2)*h)/(exp(2*Aw2)-2);

if Wid2>0 & Wid2<(2*h);
   W2 = Wid2;
else
   W2 = (2*h/pi)*(Bw2-1-log(2*Bw2-1)+((E_r-1)/(2*E_r))*(log(Bw2-1)+0.39-0.61/E_r));
end

% The value of the effective permettivity at each section:
E_eff2 = (E_r+1)/2+((E_r-1)/2)*(1/sqrt(1+12*h/W2));

% The normalized ABCD parameters @ f1
A2f1 = cos(2*pi*(l2)*f1*sqrt(E_eff2)/(c));
D2f1 = cos(2*pi*(l2)*f1*sqrt(E_eff2)/(c));
B2f1 = 1i*(Z2)*sin(2*pi*(l2)*f1*sqrt(E_eff2)/(c));
C2f1 = 1i*((Z2)^-1)*sin(2*pi*(l2)*f1*sqrt(E_eff2)/(c));

% The normalized ABCD parameters @ f2
A2f2 = cos(2*pi*(l2)*f2*sqrt(E_eff2)/(c));
D2f2 = cos(2*pi*(l2)*f2*sqrt(E_eff2)/(c));
B2f2 = 1i*(Z2)*sin(2*pi*(l2)*f2*sqrt(E_eff2)/(c));
C2f2 = 1i*((Z2)^-1)*sin(2*pi*(l2)*f2*sqrt(E_eff2)/(c));

% The normalized ABCD parameters @ f3
A2f3 = cos(2*pi*(l2)*f3*sqrt(E_eff2)/(c));
D2f3 = cos(2*pi*(l2)*f3*sqrt(E_eff2)/(c));
B2f3 = 1i*(Z2)*sin(2*pi*(l2)*f3*sqrt(E_eff2)/(c));
C2f3 = 1i*((Z2)^-1)*sin(2*pi*(l2)*f3*sqrt(E_eff2)/(c));

ABCD_2f1=[A2f1 B2f1;C2f1 D2f1]; ABCD_2f2=[A2f2 B2f2;C2f2 D2f2];
ABCD_2f3=[A2f3 B2f3;C2f3 D2f3];
```

ABCD Parameters of Z3 @ f1, f2, and f3

```
Aw3 = (Z3/60)*sqrt((E_r+1)/2)+((E_r-1)/(E_r+1))*(0.23+0.11/E_r);
Bw3 = (377*pi)/(2*Z3*sqrt(E_r));
Wid3=(8*exp(Aw3)*h)/(exp(2*Aw3)-2);

if Wid3>0 & Wid3<(2*h);
   W3 = Wid3;
else
   W3 = (2*h/pi)*(Bw3-1-log(2*Bw3-1)+((E_r-1)/(2*E_r))*(log(Bw3-1)+0.39-0.61/E_r));
end
```

```
% The value of the effective permettivity at each section:
E_eff3 = (E_r+1)/2+((E_r-1)/2)*(1/sqrt(1+12*h/W3));

% The normalized ABCD parameters @ f1
A3f1 = cos(2*pi*(l3)*f1*sqrt(E_eff3)/(c));
D3f1 = cos(2*pi*(l3)*f1*sqrt(E_eff3)/(c));
B3f1 = 1i*(Z3)*sin(2*pi*(l3)*f1*sqrt(E_eff3)/(c));
C3f1 = 1i*((Z3)^-1)*sin(2*pi*(l3)*f1*sqrt(E_eff3)/(c));

% The normalized ABCD parameters @ f2
A3f2 = cos(2*pi*(l3)*f2*sqrt(E_eff3)/(c));
D3f2 = cos(2*pi*(l3)*f2*sqrt(E_eff3)/(c));
B3f2 = 1i*(Z3)*sin(2*pi*(l3)*f2*sqrt(E_eff3)/(c));
C3f2 = 1i*((Z3)^-1)*sin(2*pi*(l3)*f2*sqrt(E_eff3)/(c));

% The normalized ABCD parameters @ f3
A3f3 = cos(2*pi*(l3)*f3*sqrt(E_eff3)/(c));
D3f3 = cos(2*pi*(l3)*f3*sqrt(E_eff3)/(c));
B3f3 = 1i*(Z3)*sin(2*pi*(l3)*f3*sqrt(E_eff3)/(c));
C3f3 = 1i*((Z3)^-1)*sin(2*pi*(l3)*f3*sqrt(E_eff3)/(c));

ABCD_3f1=[A3f1 B3f1;C3f1 D3f1]; ABCD_3f2=[A3f2 B3f2;C3f2 D3f2];
ABCD_3f3=[A3f3 B3f3;C3f3 D3f3];
```

Error Function Implementation

```
Tot_ABCD_f1 = ABCD_1f1 * ABCD_2f1 * ABCD_3f1;
Tot_ABCD_f2 = ABCD_1f2 * ABCD_2f2 * ABCD_3f2;
Tot_ABCD_f3 = ABCD_1f3 * ABCD_2f3 * ABCD_3f3;

Zin_f1      = ((Tot_ABCD_f1(1,1)*Zl)+Tot_ABCD_f1(1,2))/...
              ((Tot_ABCD_f1(2,1)*Zl)+Tot_ABCD_f1(2,2));

Zin_f2      = ((Tot_ABCD_f2(1,1)*Zl)+Tot_ABCD_f2(1,2))/...
              ((Tot_ABCD_f2(2,1)*Zl)+Tot_ABCD_f2(2,2));

Zin_f3      = ((Tot_ABCD_f3(1,1)*Zl)+Tot_ABCD_f3(1,2))/...
              ((Tot_ABCD_f3(2,1)*Zl)+Tot_ABCD_f3(2,2));

Gamma_1     = (Zin_f1 - Zs) / (Zin_f1 + Zs); % @ f1
Gamma_2     = (Zin_f2 - Zs) / (Zin_f2 + Zs); % @ f2
Gamma_3     = (Zin_f3 - Zs) / (Zin_f3 + Zs); % @ f3

Error_Fcn   = abs(Gamma_1)^2 + abs(Gamma_2)^2 + abs(Gamma_3)^2;
```

Published with MATLAB® R2016a

```
clc
close all
clear all
```

```
for ii=1:5
```

```
ii
```

The initial values of the optimization variables:

```
x0=[20e-3 20e-3 20e-3 50 50 50];
```

The lower & upper bounds:

```
xub=[60e-3 60e-3 60e-3 135 135 135];
xlb=[10e-3 10e-3 10e-3 20 20 20];
```

To Increase the number of iterations and/or reduce the tolerance:

```
options = optimset('MaxFunEvals',100000,'maxiter',2000,'TolFun',1e-60,'TolCon',1e-60,'TolX',1e-60);
```

The optimization function:

```
[x,fval,exitflag,output]=fmincon(@Tri_Band_Transformer,x0,[],[],[],[],xlb,xub,@constraint,options)
```

To save the error

```
error(ii)=fval;
results(ii,1:6)=x;
```

```
end
```

Published with MATLAB® R2016a